YANKEE ATOMIC ELECTRIC COMPANY

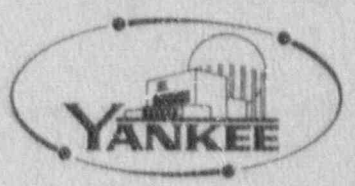

YAEC-1749

Vermont Yankee
Cycle 15
Core Performance Analysis Report

August 1990

Major Contributors:
V. Chandola
B. Y. Hubbard
M. P. LeFrancois
D. J. Morin
J. Pappas
R. C. Potter
J. D. Robichaud
R. P. Smith
K. E. St.John
R. W. Sterner
R. A. Woehlke

WPP40/10

Prepared by: M A Sironen — 8/23/90
M. A. Sironen (Date)
Nuclear Engineering Coordinator

Approved by: R A Wolfe acting manager — 8/23/90
R. J. Cacciapouti, Manager (Date)
Reactor Physics Group

Approved by: P A Bergeron — 8/23/90
P. A. Bergeron, Manager (Date)
Transient Analysis Group

Approved by: Kaver E St John for R S — 8/23/90
R. K. Sundaram, Manager (Date)
LOCA Analysis Group

Approved by: B C Slifer — 8/24/90
B. C. Slifer, Director (Date)
Nuclear Engineering Department

Yankee Atomic Electric Company
Nuclear Services Division
580 Main Street
Bolton, Massachusetts 01740

DISCLAIMER OF RESPONSIBILITY

This document was prepared by Yankee Atomic Electric Company ("Yankee"). The use of information contained in this document by anyone other than Yankee, or the Organization for which this document was prepared under contract, is not authorized and, with respect to any unauthorized use, neither Yankee nor its officers, directors, agents, or employees assume any obligation, responsibility, or liability or make any warranty or representation as to the accuracy or completeness of the material contained in this document.

ABSTRACT

This report presents design information, calculational results, and operating limits pertinent to the operation of Cycle 15 of the Vermont Yankee Nuclear Power Station. These include the fuel design and core loading pattern descriptions; calculated reactor power distributions, exposure distributions, shutdown capability, and reactivity data; and the results of safety analyses performed to justify plant operation throughout the cycle.

TABLE OF CONTENTS

TABLE OF CONTENTS
(Continued)

LIST OF FIGURES

LIST OF FIGURES
(Continued)

LIST OF TABLES

ACKNOWLEDGEMENTS

The author and major contributors would like to acknowledge the contributions to this work by U. Ansari, C. Mears and the YAEC Word Processing Center. Their assistance in preparing this document is recognized and greatly appreciated.

1.0 INTRODUCTION

This report provides information to support the operation of the Vermont Yankee Nuclear Power Station through the forthcoming Cycle 15. In this report, Cycle 15 will frequently be referred to as the Reload Cycle. The preceding Cycle 14 will frequently be referred to as the Current Cycle. The refueling between the two will involve the discharge of 128 irradiated fuel bundles and the insertion of 128 new fuel bundles. The resultant core will consist of 128 new fuel bundles and 240 irradiated fuel bundles. The General Electric Company (GE) manufactured all the bundles, except four qualification fuel bundles manufactured by Advanced Nuclear Fuels. Some of the irradiated fuel was also present in the reactor in Cycle 13. This cycle will frequently be referred to as the Past Cycle.

This report contains descriptions and analyses results pertaining to the mechanical, thermal-hydraulic, physics, and safety aspects of the Reload Cycle. The analyses assumed the reload core contained all GE bundles. Section 9.0 describes the Reload Cycle Core Component Qualification Program and its impact on the analyses. The MAPLHGR and MCPR operating limits calculated for the Reload Cycle are given in Appendix A. These limits will be included in the Core Operating Limits Report.

2.0 RECENT REACTOR OPERATING HISTORY

2.1 Operating History of the Current Cycle

The current operating cycle is Cycle 14. To date, the Current Cycle has been operated smoothly at, or near, full power with the exception of sequence exchanges, one short repair outage, two scrams, and a coastdown to the end of cycle. The operating history highlights and control rod sequence exchange schedule of the Current Cycle are found in Table 2.1.1.

2.2 Operating History of Past Applicable Cycle

The irradiated fuel in the Reload Cycle includes some fuel bundles initially inserted in Cycle 13. This Past Cycle operated smoothly at, or near, full power with the exception of sequence exchanges, two short repair outages, and a coastdown to the end of cycle. The operating history highlights of the Past Cycle are found in Table 2.2.1. The Past Cycle is described in detail in Reference 1.

TABLE 2.1.1

VY CYCLE 14 OPERATING HIGHLIGHTS

Beginning of Cycle Date	April 8, 1989
End of Cycle Date	September 1, 1990*
Weight of Uranium As-Loaded (Short Tons)	73.94
Beginning of Cycle Core Average Exposure (MWD/ST)	9195
End of Full Power Core Average Exposure (MWD/ST)	18340*
End of Cycle Core Average Exposure (MWD/ST)	19595*
Number of Fresh Assemblies	136
Number of Irradiated Assemblies	232

Control Rod Sequence Exchange Schedule:

Date	Sequence From	Sequence To
June 3, 1989	A2-1	B1-1
July 29, 1989	B1-1	A1-1
September 23, 1989	A1-1	B2-1
November 18, 1989	B2-1	A2-2
January 6, 1990	A2-2	B1-2
March 21, 1990	B1-2	A1-2
May 19, 1990	A1-2	B2-2
July 7, 1990	B2-2	A2-3

* Projected Dates and Exposures.

TABLE 2.2.1

VY CYCLE 13 OPERATING HIGHLIGHTS

Beginning of Cycle Date	October 2, 1987
End of Cycle Date	February 11, 1989
Weight of Uranium As-Loaded (Short Tons)	74.82
Beginning of Cycle Core Average Exposure (MWD/ST)	8613
End of Full Power Core Average Exposure (MWD/ST)	16901
End of Cycle Core Average Exposure (MWD/ST)	18307
Number of Fresh Assemblies	136
Number of Irradiated Assemblies	232

Control Rod Sequence Exchange Schedule:

Date	Sequence From	Sequence To
December 5, 1987	A2-1	B1-1
January 30, 1988	B1-1	A1-1
March 19, 1988	A1-1	B2-1
April 30, 1988	B2-1	A2-2
July 2, 1988	A2-2	B1-2
August 24, 1988	B1-2	A1-2
October 29, 1988	A1-2	B2-2

3.0 RELOAD CORE DESIGN DESCRIPTION

3.1 Core Fuel Loading

The Reload Cycle core will consist of both new and irradiated assemblies. All the assemblies have bypass flow holes drilled in the lower tie plate. Table 3.1.1 characterizes the core by fuel type, batch size, and first cycle loaded. A description of the fuel is found in Reference 2.

3.2 Design Reference Core Loading Pattern

The Reload Cycle assembly locations are indicated on the map in Figure 3.2.1. For the sake of legibility only the lower right quadrant is shown. The other quadrants are mirror images with bundles of the same type having nearly identical exposures. The bundles are identified by the reload number in which they were first introduced into the core. If any changes are made to the loading pattern at the time of refueling, they will be evaluated under 10CFR50.59. The final loading pattern with specific bundle serial numbers will be supplied in the Startup Test Report.

3.3 Assembly Exposure Distribution

The assumed nominal exposure on the fuel bundles in the Reload Cycle design reference loading pattern is given in Figure 3.2.1. To obtain this exposure distribution, the Past Cycle was depleted with the SIMULATE-3 model [3-4] using actual plant operating history. For the Current Cycle, plant operating history was used through January 10, 1990. Beyond this date, the exposure was accumulated using a best-estimate rodded depletion analysis to End of Full Power Life (EOFPL) followed by a projected coastdown to End of Cycle (EOC).

Table 3.3.1 gives the assumed nominal exposure on the Current Cycle and the Beginning of Cycle (BOC) core average exposure that results from the shuffle into the Reload Cycle loading pattern. The Reload Cycle EOFPL core average exposure and cycle capability are provided.

TABLE 3.1.1

ASSUMED VY CYCLE 15 FUEL BUNDLE TYPES AND NUMBERS

	Fuel Designation	Reload Designation	Cycle Loaded	Number
Irradiated	BP8DRB299	R12	13	104
	BD326B	R13A	14	88
	BD324B	R13B	14	48
New	BP8DWB311-10GZ	R14A	15	64
	BP8DWB311-11GZ	R14B	15	64

TABLE 3.3.1

DESIGN BASIS VY CYCLE 14 AND CYCLE 15 EXPOSURES

Assumed End of Current Cycle Core Average Exposure	19.59 GWD/ST
Assumed Beginning of Reload Cycle Core Average Exposure	10.71 GWD/ST
Haling Calculated End of Full Power Life Reload Cycle Core Average Exposure	19.76 GWD/ST
Reload Cycle Full Power Exposure Capability	9.05 GWD/ST

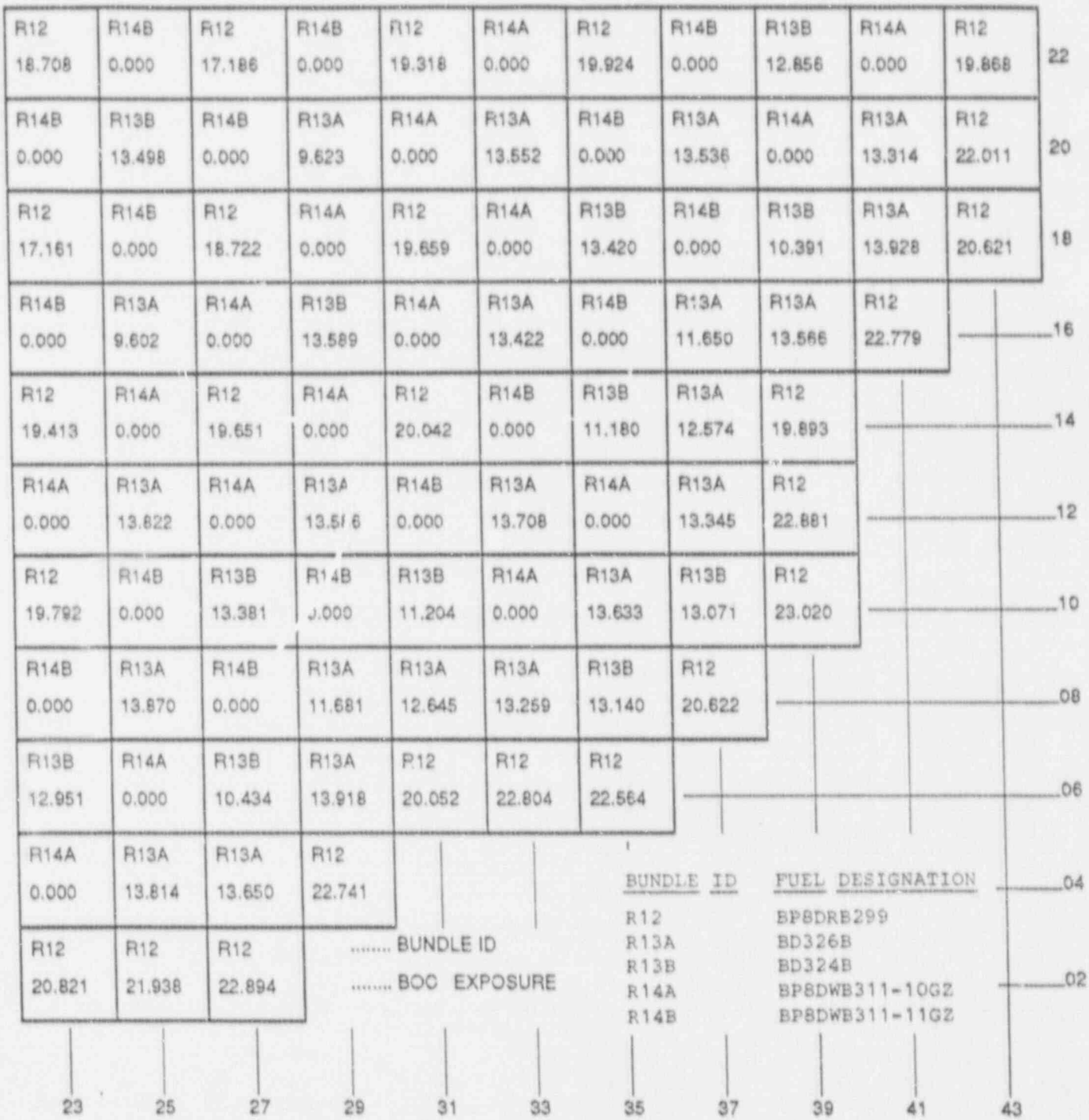

FIGURE 3.2.1

VY Cycle 15 Design Reference Loading Pattern, Lower Right Quadrant

WPP40/10

4.0 FUEL MECHANICAL AND THERMAL DESIGN

4.1 Mechanical Design

Most of the fuel to be inserted into the Reload Cycle was fabricated by GE. The major mechanical design parameters are given in Table 4.1.1 and Reference 2. Several design changes have been incorporated in the Reload Cycle fuel design. The new fuel bundles differ from the irradiated bundles in the following ways: 1) the average bundle enrichment has been changed to 3.11 w/o U-235; 2) the ferrule spacer is used; and 3) the number of water rods has been changed to one large central rod. Detailed descriptions of the fuel rod mechanical design and mechanical design analyses are provided in Reference 2. These design analyses remain valid with respect to the Reload Cycle operation. Mechanical and chemical compatibility of the fuel bundles with the in-service reactor environment is also addressed in Reference 2.

4.2 Thermal Design

The fuel thermal effects calculations were performed using the FROSSTEY-2 computer code [5]. The FROSSTEY-2 code calculates pellet-to-cladding gap conductance and fuel temperatures from a combination of theoretical and empirical models which include fuel and cladding thermal expansion, fission gas release, pellet swelling, pellet densification, pellet cracking, and fuel and cladding thermal conductivity.

The thermal effects analysis included the calculation of fuel temperatures and fuel cladding gap conductance under nominal core steady state and peak linear heat generation rate conditions. Figure 4.2.1 provides the core average response of gap conductance. These calculations integrate the responses of individual fuel batch average operating histories over the core average exposure range of the Reload Cycle. The gap conductance values are weighted axially by power distributions and radially by volume. The core-wide gap conductance values for the RETRAN system simulations, described in Sections 7.1 through 7.3, are from this data set at the corresponding exposure statepoints.

The gap conductance values input to the hot channel calculations (Section 7.1) were evaluated for the given fuel bundle type as a function of the assembly exposure. The calculation assumed a 1.4 chopped cosine axial power shape with the peak power node running at the maximum average planar linear heat generation rate (MAPLHGR) limit defined in Reference 6. Figures 4.2.2 and 4.2.3 provide the hot channel response of gap conductance. In Figures 4.2.2 and 4.2.3, "planar exposure" refers to the exposure of the node operating at the MAPLHGR limit. Gap conductance values for the hot channel analysis were extracted from the figures using the limiting bundle exposure of any minimum critical power ratio (MCPR) limiting bundle within the exposure interval of interest. The SIMULATE rodded depletion (Section 5.1.2) provides predictions of both limiting MCPR and the associated bundle exposure for the entire cycle.

Table 4.2.1 provides the core average and hot channel gap conductance values used in the transient analyses (Section 7.1). The values for gap conductance are slightly higher than those calculated in previous cycles for the following reasons: 1) the bundles in the core now have the larger diameter pellet, and 2) the new bundle may operate at a higher, relative power level as provided by the MAPLHGR limits.

Fuel rod local linear heat generation rates (LHGR) at fuel centerline incipient melt and 1% cladding plastic strain as a function of local axial segment exposure for the peak gadolinia concentrations used in Vermont Yankee fuel bundles were calculated. These values are displayed in Table 4.2.2. Initial conditions assumed that fuel rods operated at the local segment power level of the maximum allowable LHGR prior to the power increase.

4.3 Operating Experience

All irradiated fuel bundles scheduled to be reinserted in the Reload Cycle have operated as expected in Past Cycles of Vermont Yankee. Off-gas measurements in the Current Cycle indicate that a number of fuel rod failures may have occurred. Vermont Yankee is planning to identify the failed rods during the outage.

TABLE 4.1.1

NOMINAL FUEL MECHANICAL DESIGN PARAMETERS

	Fuel Types		
	Irradiated		New
	Twice-Burned	Once-Burned	
Fuel Bundle*			
Bundle Types	BP8X8R	BP8X8EB	GE8X8NB
Vendor Designation (Table 3.1.1)	BP8DRB299	BD324B and BD326B	BP8DWB311-10GZ and BP8DWB311-11GZ
Initial Enrichment, w/o U235	2.99	3.24 and 3.26	3.11
Rod Array	8X8	8X8	8X8
Fuel Rods per Bundle	62	60	60
Outer Fuel Channel			
Material	Zr-4	Zr-4	Zr-2
Wall Thickness, inches	0.080	0.080	0.080

*Complete bundle, rod, and pellet descriptions are found in Reference 2.

TABLE 4.2.1

VY CYCLE 15 GAP CONDUCTANCE VALUES USED IN TRANSIENT ANALYSES

		Irradiated Fuel Bundles		New Fuel Bundles	
Cycle Exposure Statepoint (MWD/ST)	Core Average Gap Conductance (BTU/Hr-Ft^2- ^{o}F)	Hot Channel Bundle Exposure (MWD/ST)	Hot Channel[1] Gap Conductance (BTU/Hr-Ft^2 - ^{o}F)	Hot Channel Bundle Exposure (MWD/ST)	Hot Channel[2] Gap Conductance (BTU/Hr-Ft^2 - ^{o}F)
BOC15	2740	10746[3]	4750	7788	4880
EOFPL15-2000 MWD/ST	4000	17269	4490	8576	5010
EOFPL15-1000 MWD/ST	4090	18608	4370	10005[3]	5080
EOFPL15	4320	19756	4290	10005[3]	5080

NOTES

(1) Hot channel gap conductance values are derived for the BD324B fuel type because it is conservative compared to the other fuel types.

(2) Hot channel gap conductance values are derived for the BP8DWB311-10GZ.

(3) Taken as the highest point in the exposure range.

TABLE 4.2.2

PEAK LINEAR HEAT GENERATION RATES CORRESPONDING TO INCIPIENT FUEL CENTERLINE MELTING AND 1% CLADDING PLASTIC STRAIN(1)

		0.0 w/o Gd_2O_3		4.0 w/o Gd_2O_3	
	Exposure (MWD/MT)	Melt (kW/ft)	1% ϵ_p (kW/ft)	Melt (kW/ft)	1% ϵ_p (kW/ft)
Fuel Type BP8x8R					
BP8DRB299	0	24.0	24.0	21.5	24.0
	25,000	24.0	24.0	20.5	20.5
	50,000	23.5	15.5	19.0	12.0

		0.0 w/o Gd_2O_3		5.0 w/o Gd_2O_3	
	Exposure (MWD/MT)	Melt (kW/ft)	1% ϵ_p (kW/ft)	Melt (kW/ft)	1% ϵ_p (kW/ft)
Fuel Type GE8X8EB					
BD326B	0	24.0	24.0	21.0	23.0
and	25,000	24.0	24.0	20.0	20.0
BD324B	50,000	24.0	16.0	19.0	12.0

		0.0 w/o Gd_2O_3		4.0 w/o Gd_2O_3	
	Exposure (MWD/MT)	Melt (kW/ft)	1% ϵ_p (kW/ft)	Melt (kW/ft)	1% ϵ_p (kW/ft)
Fuel Type GE8X8NB					
BP8DWB311-11GZ	0	24.0	.0	21.0	23.5
BP8DWB311-10GZ	25,000	24.0	.0	20.0	20.0
	50,000	20.5	. 5	16.5	11.0

NOTE

(1) Peak linear heat generation rates shown are minimum bounding values to the occurrence of the given condition.

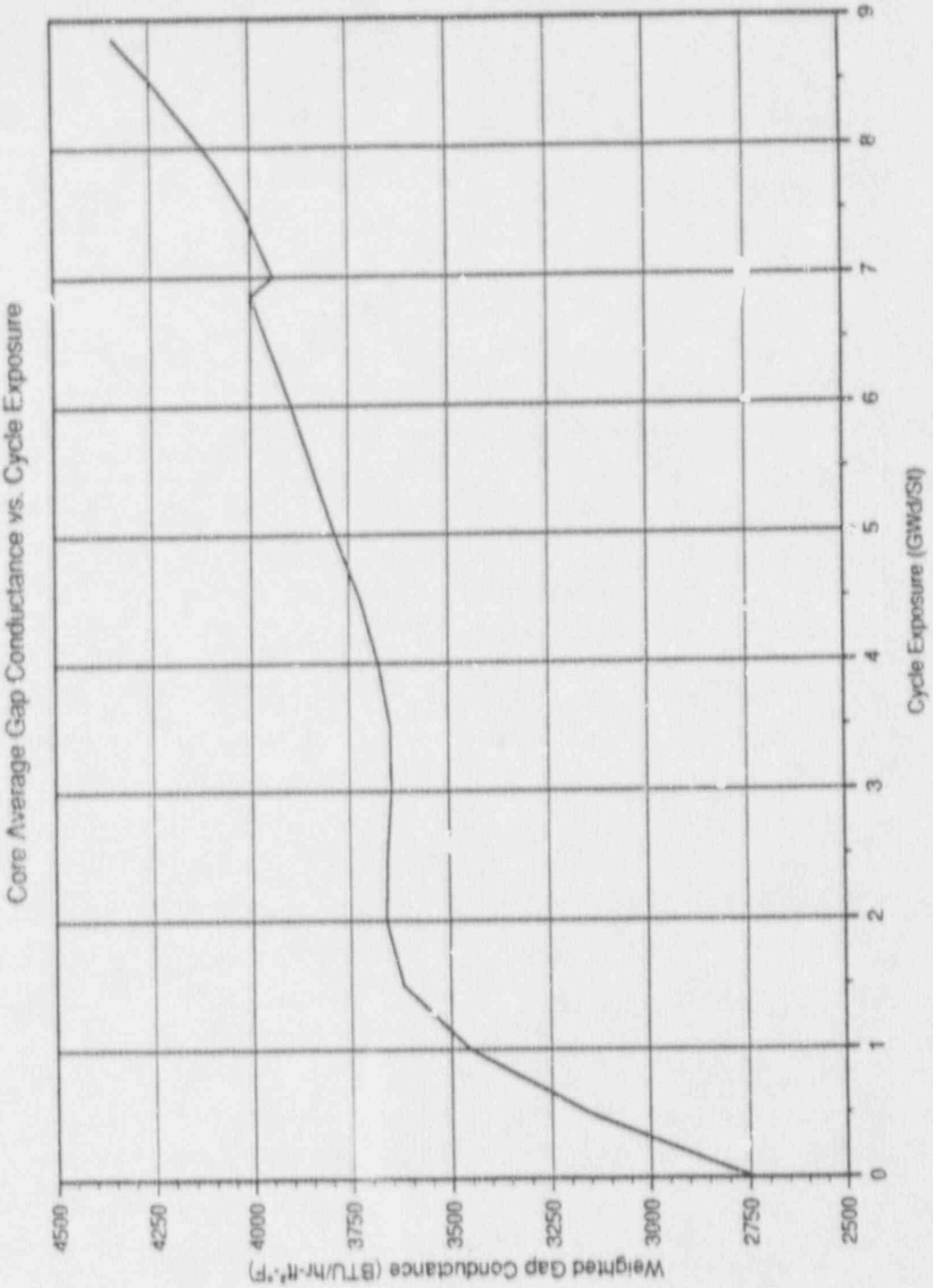

FIGURE 4.2.1

VY Cycle 15 Core Average Gap Conductance Versus Cycle Exposure

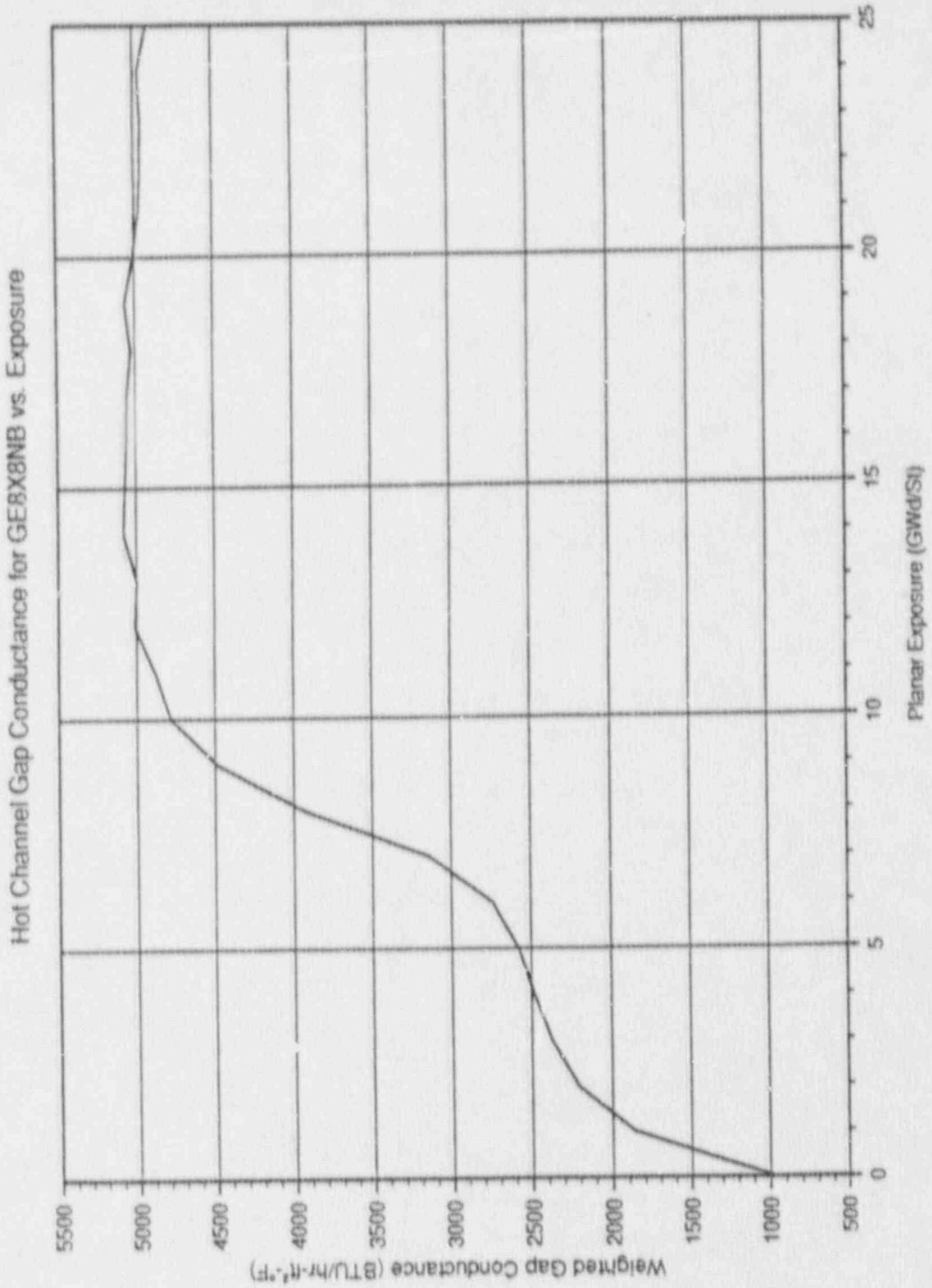

FIGURE 4.2.2

VY Hot Channel Gap Conductance for GE8X8NB Versus Exposure

WPP4J/10

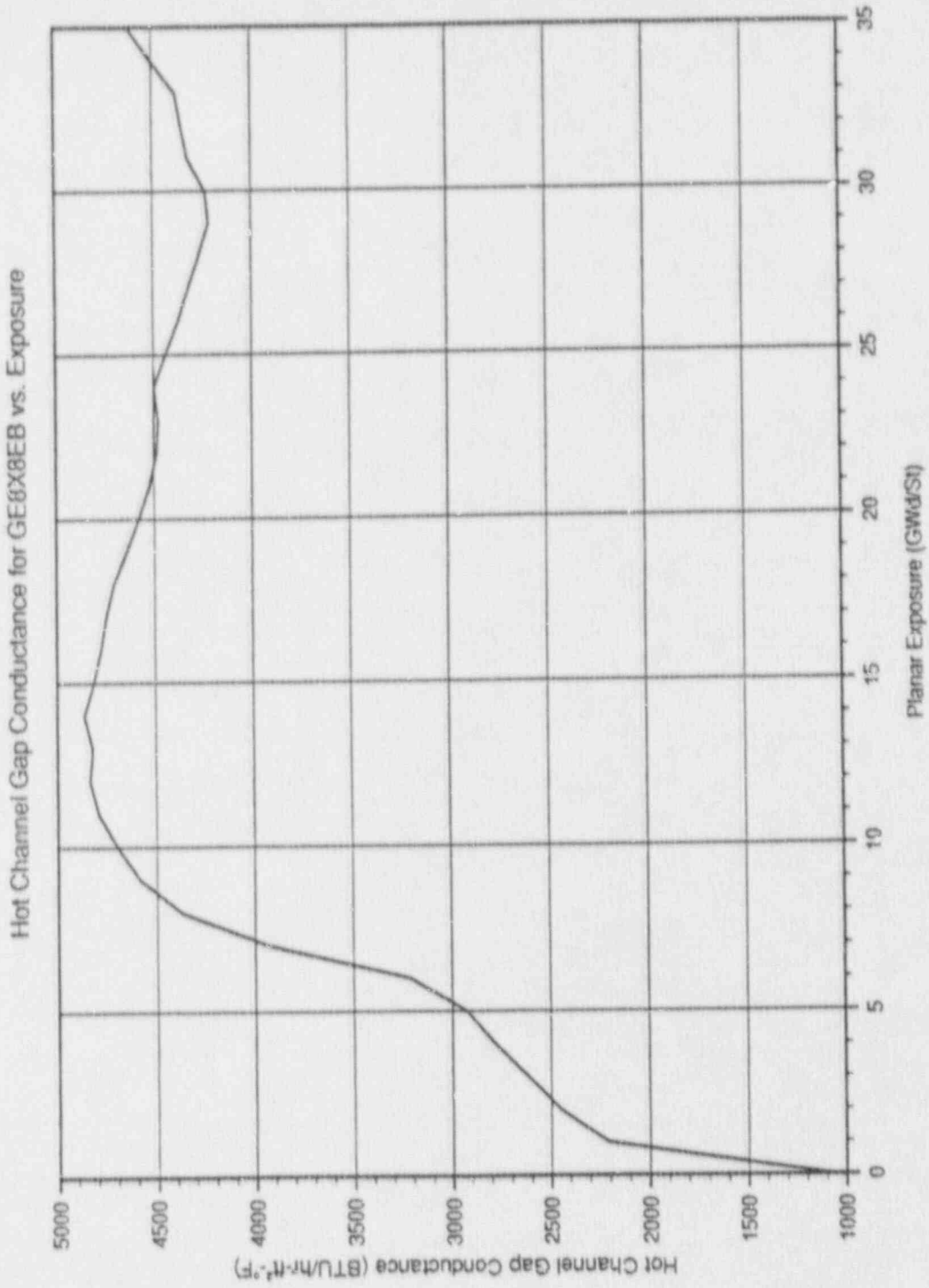

FIGURE 4.2.3

VY Hot Channel Gap Conductance for GE8X8EB Versus Exposure

5.0 NUCLEAR DESIGN

5.1 Core Power Distributions

The Reload Cycle was depleted using SIMULATE-3 [3-4] to give both a rodded depletion and an All Rods Out (ARO) Haling depletion.

5.1.1 Haling Power Distribution

The Haling depletion serves as the basis for defining core reactivity characteristics for most transient evaluations. This is primarily because its flat power shape has conservatively weak scram characteristics.

The Haling power distribution is calculated in the ARO condition. The Haling iteration converges on a self-consistent power and exposure distribution for the burnup step to EOFPL. In principle, this should provide the overall minimum peaking power shape for the cycle. During the actual cycle, flatter power distributions might occasionally be achieved by shaping with control rods. However, such shaping would leave underburned regions in the core which would peak at another point in time. Figures 5.1.1 and 5.1.2 give the Haling radial and axial average power distributions for the Reload Cycle.

5.1.2 Rodded Depletion Power Distribution

The rodded depletion was used to evaluate the mislocated bundle error and the rod withdrawal error because it provides initializing rod patterns and it provides more realistic predictions of initial CPR values. It was also used in the rod drop worth and shutdown margin calculations because it burns the top of the core more realistically than the Haling depletion.

To generate the rodded depletion, control rod patterns were developed which give critical eigenvalues at each point in the cycle and peaking similar to the Haling calculation. The resulting patterns were frequently more peaked than the Haling, but were below expected operating limits. However, as stated

above, the underburned regions of the core can exhibit peaking in excess of the Haling peaking when pulling ARO at EOFPL. Figures 5.1.3 and 5.1.4 give the ARO at EOFPL power distributions for the Reload Cycle rodded depletion. Note, in Figure 5.1.4, that the average axial power at ARO for the rodded depletion is more bottom peaked than the Haling (Figure 5.1.2). The rodded depletion would result in better scram characteristics at EOFPL.

5.2 Core Exposure Distributions

The Reload Cycle exposures are summarized in Table 3.3.1. The projected BOC radial exposure distribution for the Reload Cycle is given in Figure 3.2.1. The Haling calculation produced the EOFPL radial exposure distribution given in Figure 5.2.1. Since the Haling power shape is constant, it can be held fixed by SIMULATE-3 to give the exposure distributions at various mid-cycle points. BOC, EOFPL-2000 MWD/ST, EOFPL-1000 MWD/ST, and EOFPL exposure distributions were used to develop reactivity input for the core wide transient analyses.

The rodded depletion differs from the Haling during the cycle because the rods shape the power differently. However, rod sequences are swapped frequently and the overall exposure distribution at end of cycle is similar to the Haling. Figure 5.2.2 gives the EOFPL radial exposure distribution for the Reload Cycle rodded depletion.

5.3 Cold Shutdown Margin

Technical Specifications [7] state that, for sufficient shutdown margin, the core must be subcritical by at least 0.25% ΔK + R (defined below) with the strongest worth control rod withdrawn. Using SIMULATE-3, a search was made for the strongest worth control rod at various exposures in the cycle. This is necessary because rod worths change with exposure on adjacent assemblies. Then the cold K_{eff} with the strongest rod out was calculated at BOC and at the end of each control rod sequence. Subtracting each cold K_{eff} with the strongest rod out from the cold critical K_{eff} eigenvalue defines the shutdown margin as a function of exposure. Figure 5.3.1 shows the results.

The cold critical eigenvalue K_{eff} was defined as the average calculated critical eigenvalue minus a 95% confidence level uncertainty. Then all cold results were normalized to make the critical K_{eff} eigenvalue equal to 1.000.

Because the local reactivity may increase with exposure, the shutdown margin (SDM) may decrease. To account for this and other uncertainties, the value R is calculated. R is defined as R_1 plus R_2. R_1 is the difference between the cold K_{eff} with the strongest rod out at BOC and the maximum cold K_{eff} with the strongest rod out in the cycle. R_2 is a measurement uncertainty in the demonstration of SDM associated with the manufacture of past control blades. It is presently set at .07% ΔK. The shutdown margin results are summarized in Table 5.3.1.

5.4 Standby Liquid Control System Shutdown Capability

The shutdown capability of the Standby Liquid Control System (SLCS) is designed to bring the reactor from full power to cold, ARO, xenon free shutdown with at least 5% ΔK margin. Using SIMULATE-3, the ppm of boron was adjusted until the K_{eff} reached the cold critical K_{eff} minus .05. Each case assumed cold, xenon-free conditions, with All Rods Out. The Reload Cycle was searched to find the most reactive point in the cycle. This analysis found that the plant would be subcritical by 5% ΔK at the worst point in cycle with less than the 800 ppm of boron required by VY Technical Specifications. Table 5.4.1 lists the amount of boron concentration and the corresponding shutdown capability of the SLCS.

5.5 Maximum K_∞ for the Spent Fuel Pool

Section 5.5E of the Technical Specification requires that the K_∞ for any bundle stored in either the new fuel vault or the spent fuel pool not exceed 1.31 to ensure compliance with the K_{eff} safety limit of 0.95. The bundles used in the Reload Cycle do not exceed the specifications in Section 5.5E, as shown in Table 5.5.1. These values are obtained from CASMO-3G [8].

TABLE 5.3.1

VY CYCLE 15
K_{eff} VALUES AND SHUTDOWN MARGIN CALCULATION

Cold Critical K_{eff} Eigenvalue	1.0000
BOC K_{eff} - Controlled With Strongest Worth Rod Withdrawn	.9808
Cycle Minimum Shutdown Margin Occurs at BOC With Strongest Worth Rod Withdrawn	1.92% ΔK
R_1, Maximum Increase in Cold K_{eff} With Exposure	.00% ΔK

TABLE 5.4.1

VY CYCLE 15
STANDBY LIQUID CONTROL SYSTEM SHUTDOWN CAPABILITY

ppm of Boron	Shutdown Margin
609	5.0% ΔK
800	8.55% ΔK

TABLE 5.5.1

VY CYCLE 15
MAXIMUM COLD K_∞ OF ANY ENRICHED SEGMENT

Bundle Type	Maximum K_∞
BP8DRB299	1.19
BD324B	1.20
BD326B	1.20
BP8DWB311-10GZ	1.20
BP8DWB311-11GZ	1.20

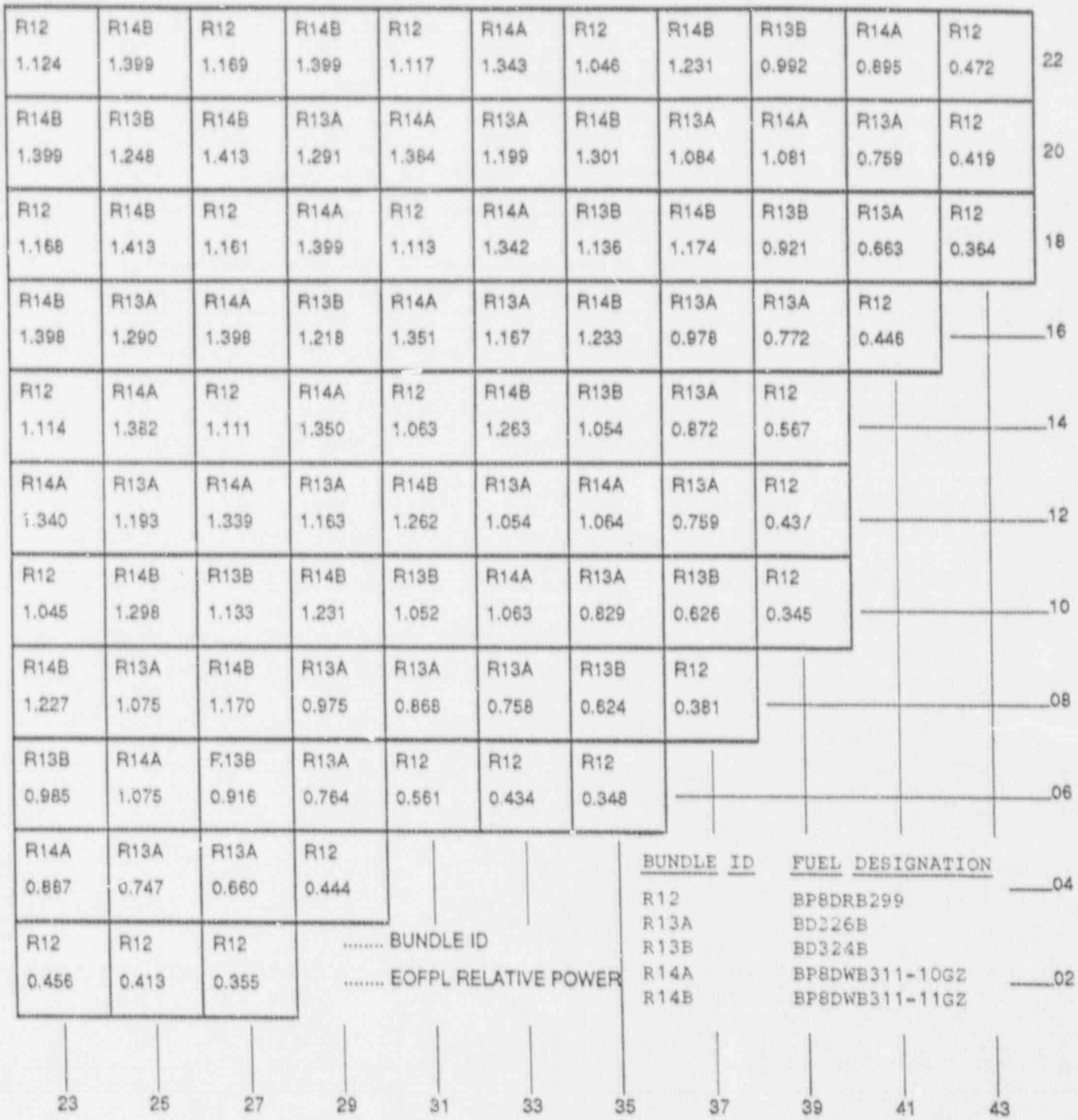

FIGURE 5.1.1

VY Cycle 15 Haling Depletion, EOFPL Bundle Average Relative Powers

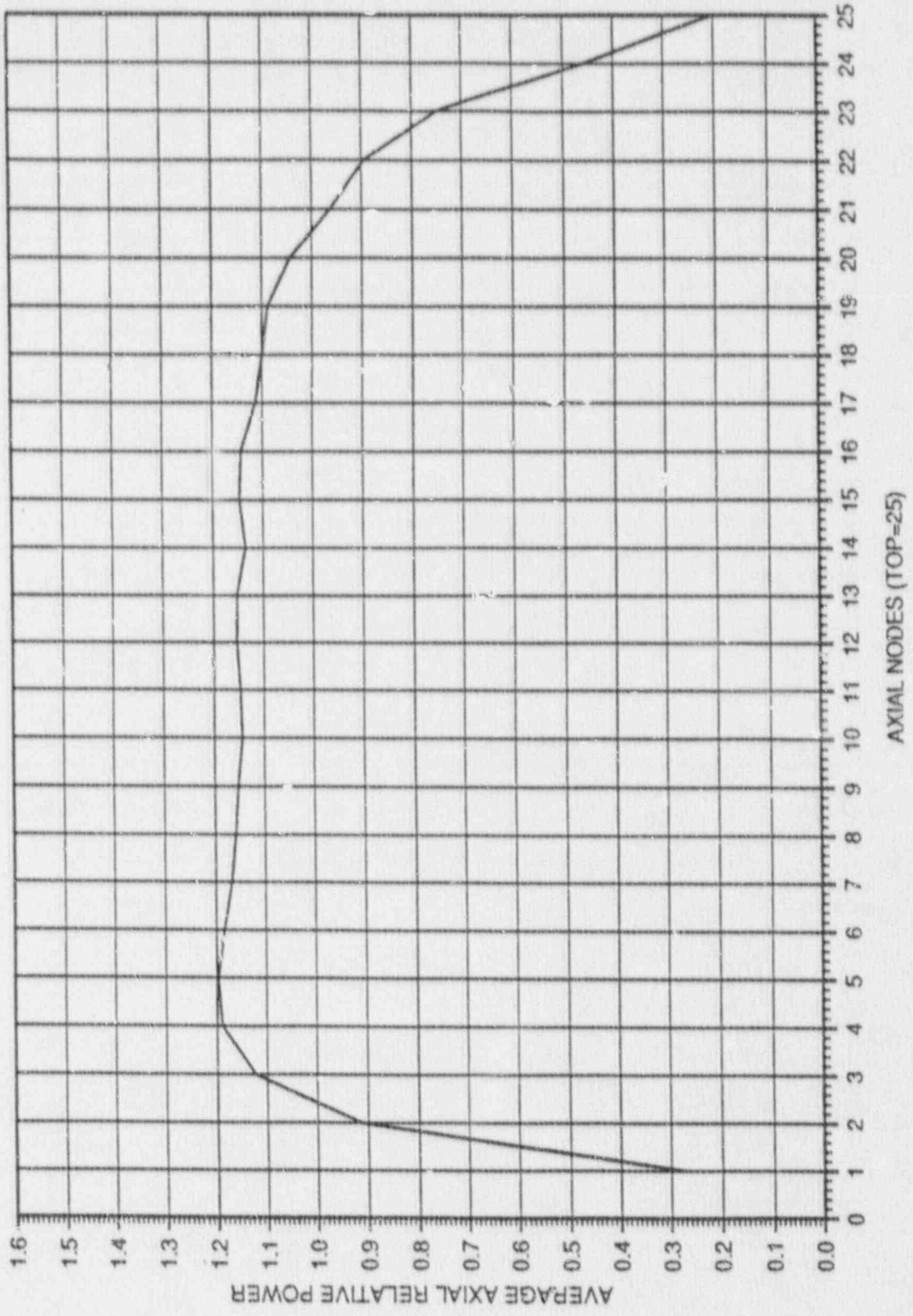

FIGURE 5.1.2

VY Cycle 13 Haling Depletion, EOFPL Core Average Axial Power Distribution

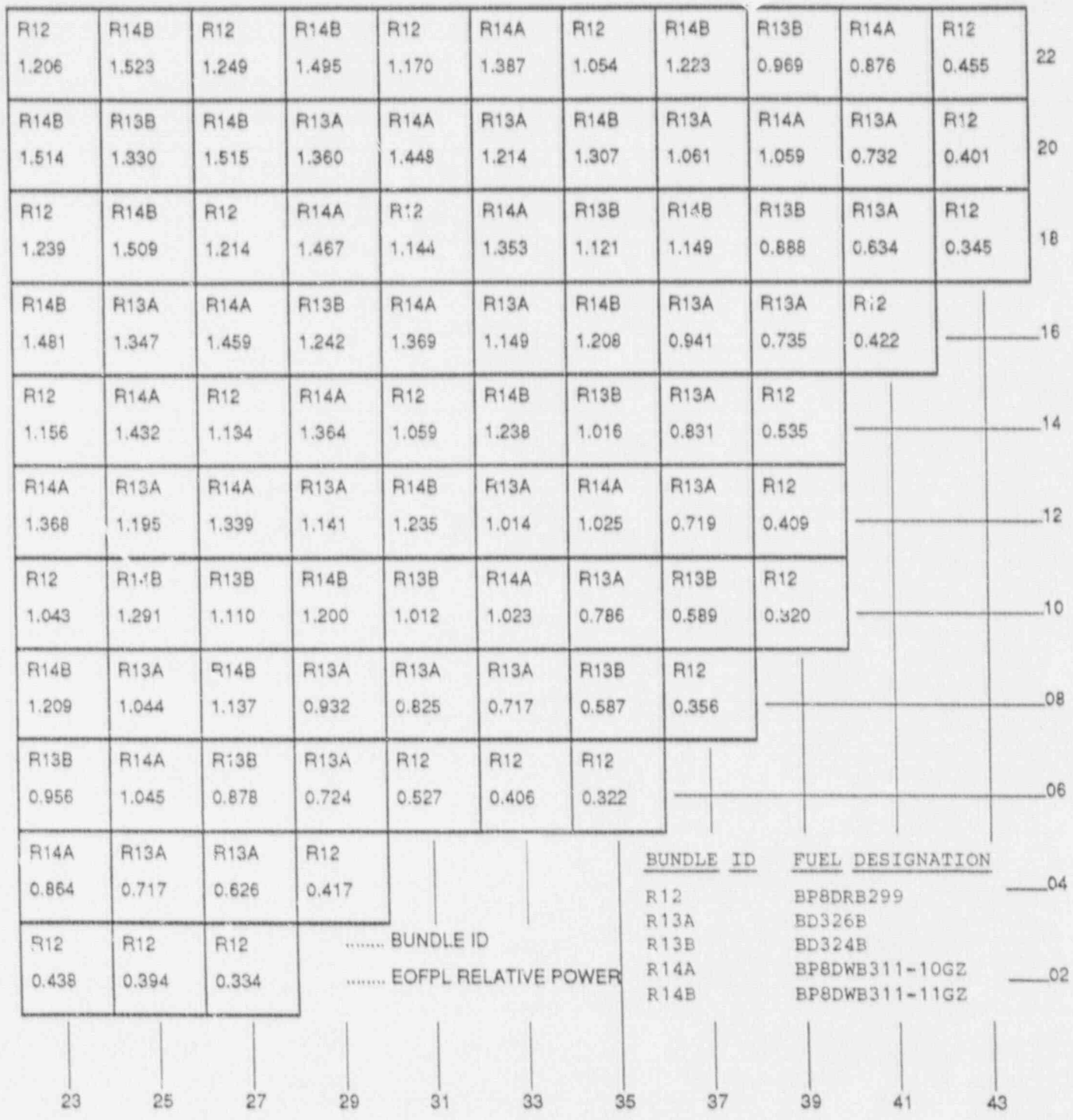

FIGURE 5.1.3

VY Cycle 15 Rodded Depletion - ARO at EOFPL,
Bundle Average Relative Powers

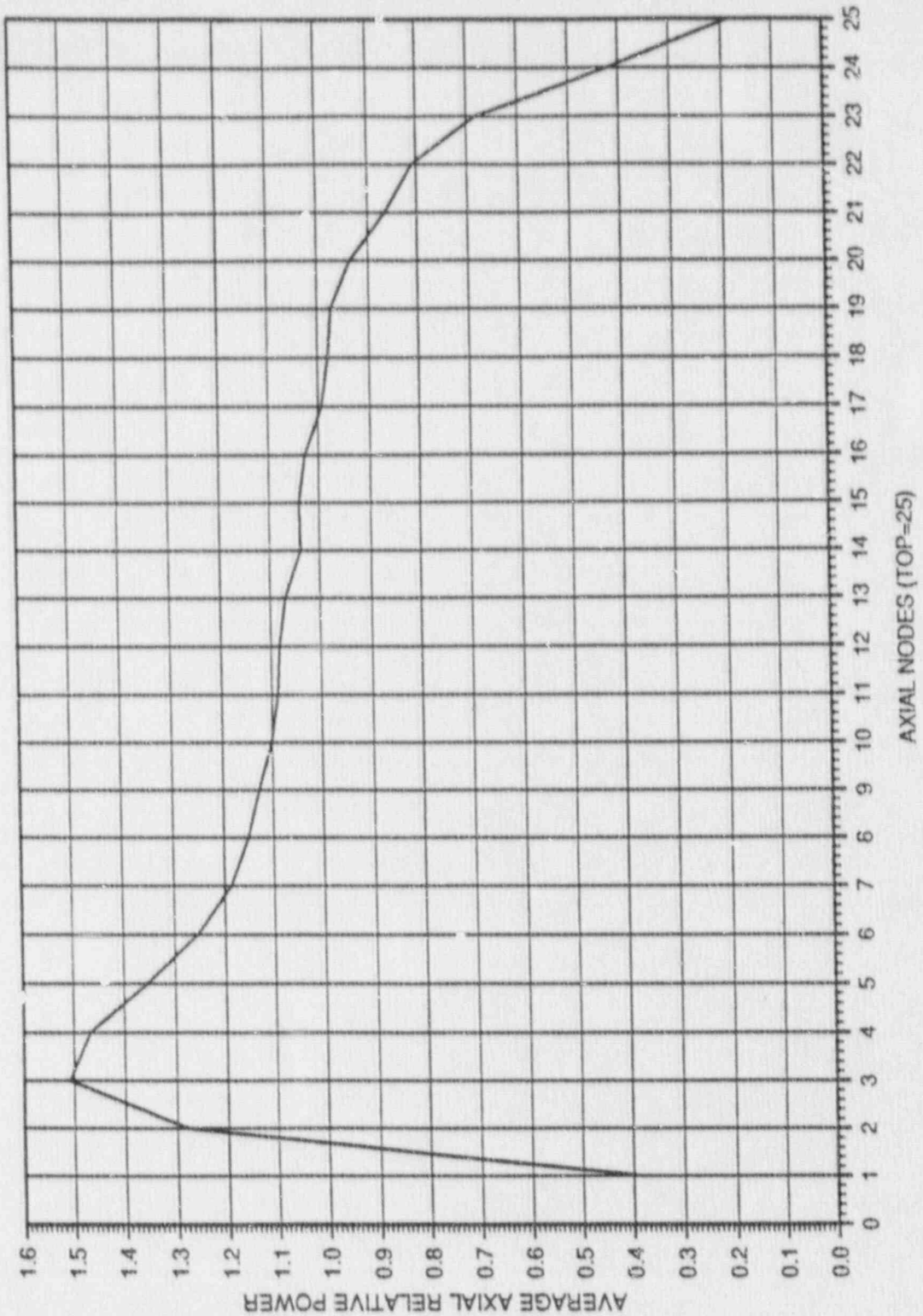

FIGURE 5.1.4

VY Cycle 15 Rodded Depletion - ARO at EOFPL,
Core Average Axial Power Distribution

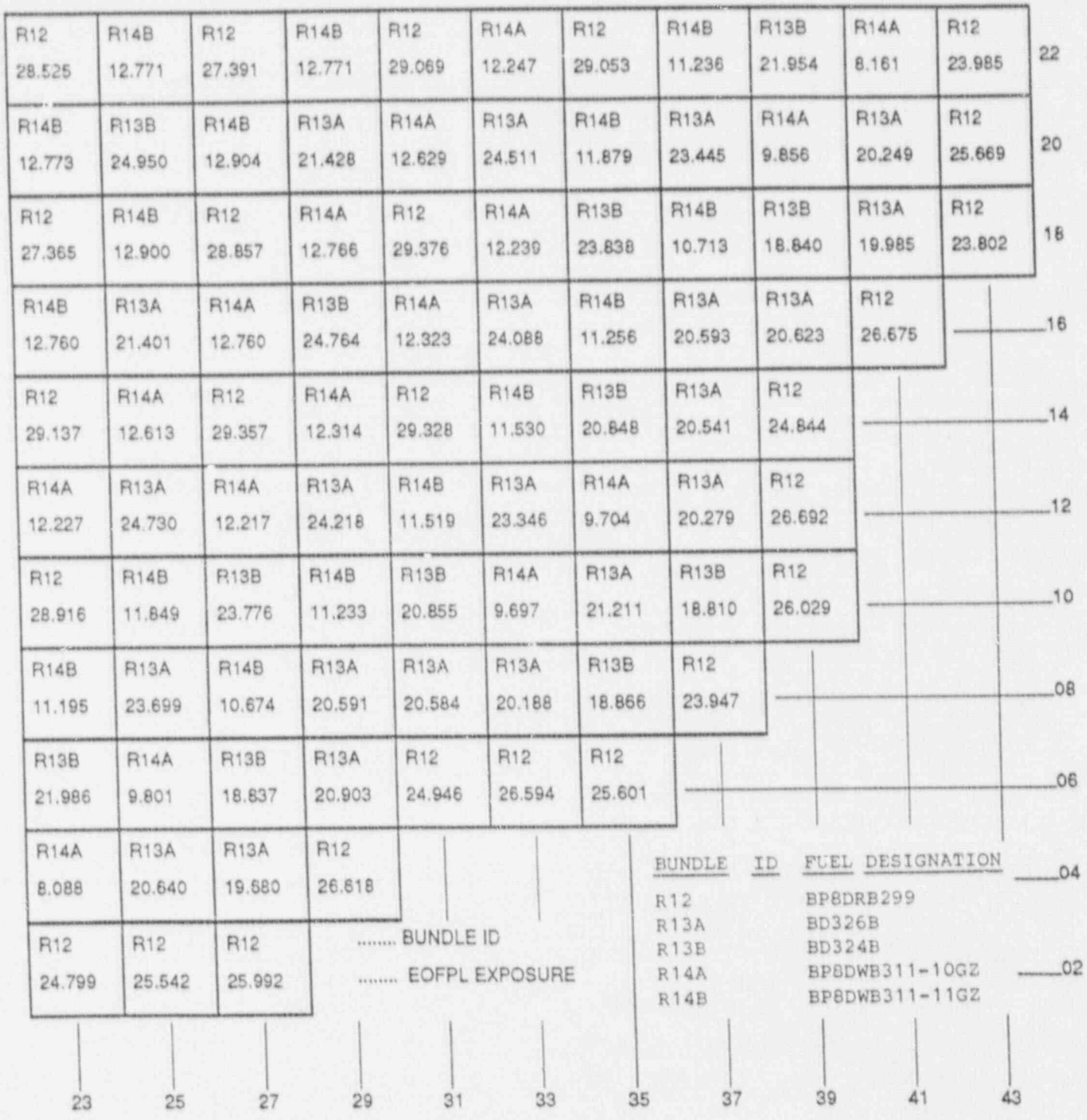

FIGURE 5.2.1

VY Cycle 15 Haling Depletion, EOFPL Bundle Average Exposures

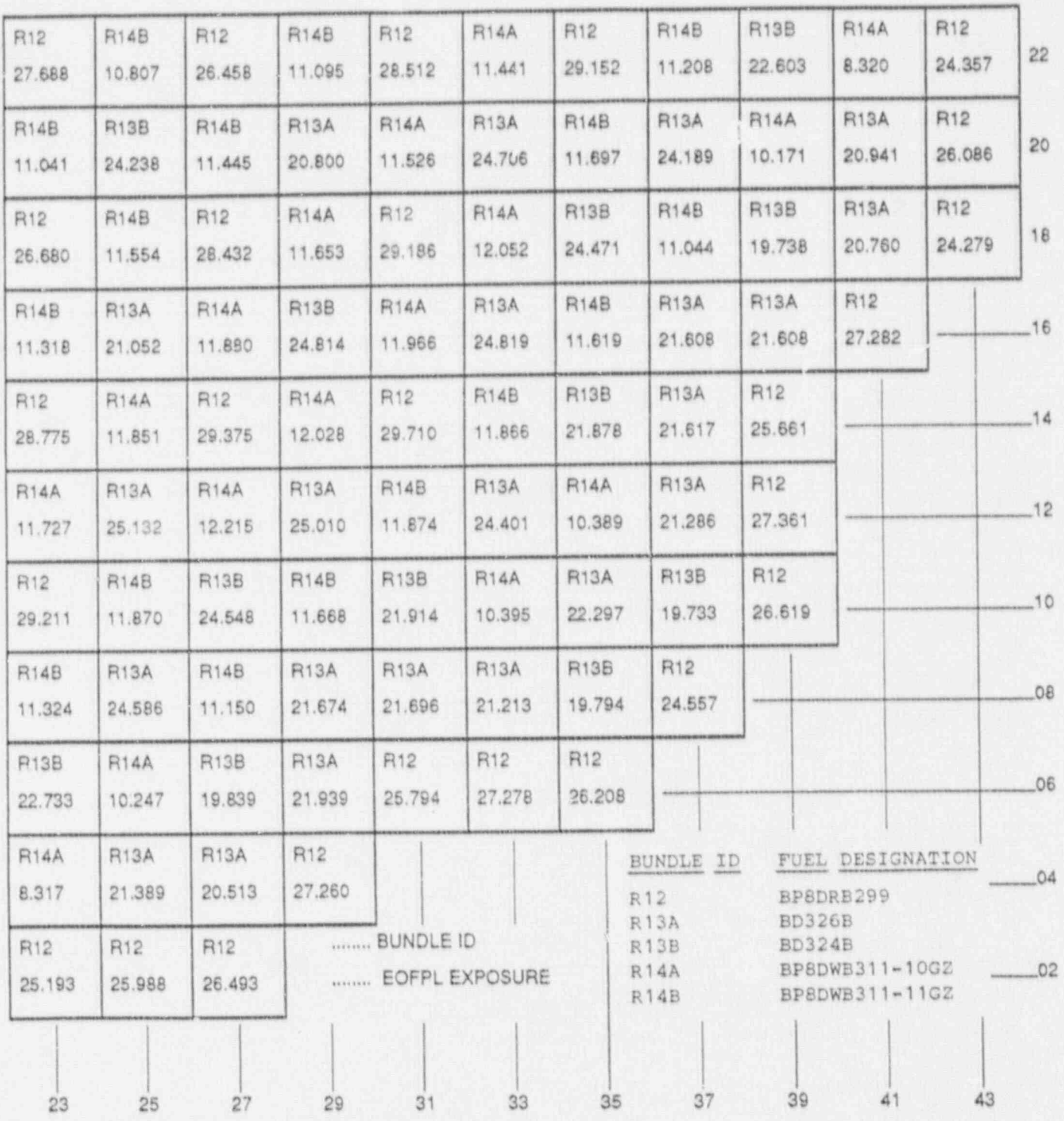

FIGURE 5.2.2

VY Cycle 15 Rodded Depletion, EOFPL Bundle Average Exposures

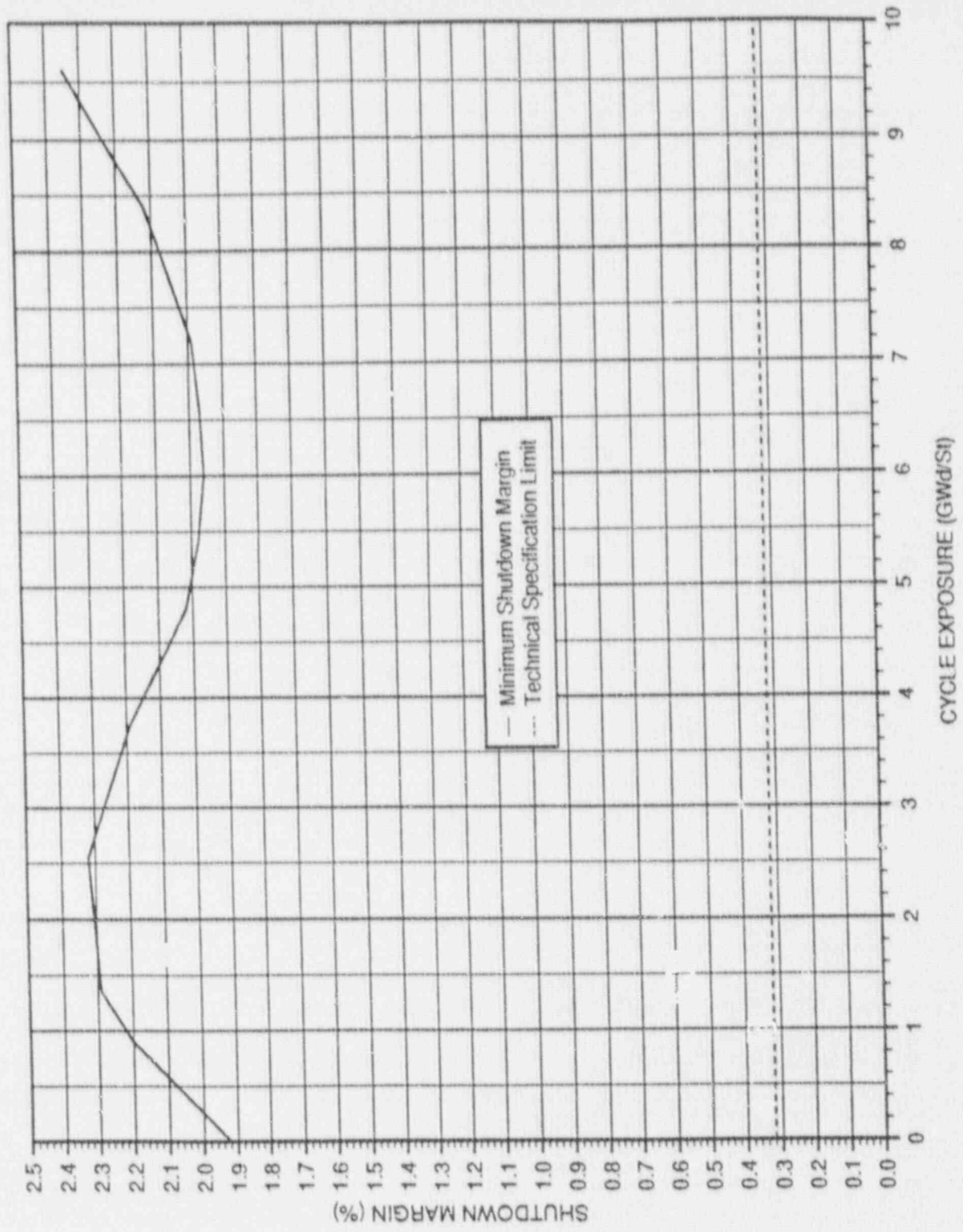

FIGURE 5.3.1

VY Cycle 15 Cold Shutdown ΔK in Percent Versus Cycle Exposure

6.0 THERMAL-HYDRAULIC DESIGN

6.1 Steady-State Thermal Hydraulics

Core steady-state thermal-hydraulic analyses for the Reload Cycle were performed using the FIBWR [9-11] computer code. The FIBWR code incorporates a detailed geometrical representation of the complex flow paths in a BWR core, and explicitly models the leakage flow to the bypass region and water rod flow. The FIBWR geometric models for each GE bundle type were benchmarked against vendor-supplied and plant thermal-hydraulic information.

Using the fuel bundle geometric models, a power distribution calculated by SIMULATE-3 [3-4] and core inlet enthalpy, the FIBWR code calculates the core pressure drop and total bypass flow for a given total core flow. The core pressure drop and total bypass flow predicted by the FIBWR code were then used in setting the initial conditions for the system transient analysis model.

6.2 Reactor Limits Determination

The objective for normal operation and anticipated transient events is to maintain nucleate boiling. Avoiding a transition to film boiling protects the fuel cladding integrity. The Fuel Cladding Integrity Safety Limit (FCISL) for Vermont Yankee is a Critical Power Ratio (CPR) of 1.07 [2]. CPR is defined as the ratio of the critical power (bundle power at which some point within the assembly experiences onset of boiling transition) to the operating bundle power. Thermal margin is stated in terms of the minimum value of the Minimum Critical Power Ratio (MCPR) which corresponds to the most limiting fuel assembly in the core. Both the transient (safety) and normal operating thermal limits, in terms of MCPR, are derived with the GEXL-Plus correlation as described in Reference 12.

The Reload Cycle fuel has Linear Heat Generation Rate (LHGR) limits of 13.4 kW/ft for Bundle Type BP8X8R, 14.4 kW/ft for Bundle Types GE8X8EB and GE8X8NB. The basis for these Maximum LHGR (MLHGR) limits can be found in Reference 2.

The Reload Cycle fuel has Average Planar Linear Heat Generation Rate (APLHGR) limits shown in Appendix A. The Maximum APLHGR (MAPLHGR) values are the most limiting composite of the fuel mechanical analysis MAPLHGRs and the LOCA analysis MAPLHGRs. The fuel mechanical design analysis, using the methods in Reference 2, demonstrate that all fuel rods in a lattice, operating at the bounding power history, meet the fuel design limits specified in Reference 2. The transients described in Section 7.0 were analyzed to verify that design criteria in the mechanical design analysis methods was not exceeded during the transient. The LOCA analysis is described in Section 8.0.

7.0 ACCIDENT ANALYSIS

7.1 Transient Analysis

Transient simulations are performed to assess the impact of certain transients on the heat transfer characteristics of the fuel. It is the purpose of the analysis to determine the MCPR operating limit, such that the FCISL is not violated for the transients considered.

7.1.1 Methodology

The analysis requires two types of simulations. A system level simulation is performed to determine the overall plant response. Transient core inlet and exit conditions and normalized power from the system level calculation are then used to perform detailed thermal-hydraulic simulations of the fuel, referred to as "hot channel calculations." The hot channel simulations provide the bundle transient ΔCPR (the initial bundle CPR minus the MCPR experienced during the transient).

The system level simulations are performed with the model documented in References 13 through 15.

The hot channel calculations are performed with the RETRAN [16-17] and TCPYA01 [18,11,15] computer codes. The GEXL-Plus correlation [12] is used in TCPYA01 to evaluate critical power ratio. The calculational procedure is outlined below.

The hot channel transient ΔCPR calculations employ a two-part process, as illustrated by the flow chart in Figure 7.1.1. The first part involves a series of steady-state analyses performed with the FIBWR, RETRAN, and TCPYA01 computer codes. The FIBWR analyses utilize a one-channel model for each fuel type being analyzed, with bypass and water rod flow also modeled. The steady-state FIBWR analyses were performed at several power levels with other

conditions (i.e., core pressure drop, system pressure, and core inlet enthalpy) held constant. The FIBWR code result is an active channel flow (AF) and bypass flow (BPF) for each active channel power (AP).

The FIBWR conditions for channel power, channel flow, and bypass flow were then used as input to steady-state RETRAN/TCPYA01 hot channel calculations. Other assumptions are consistent with those in the FIBWR analysis. The Initial Critical Power Ratio (ICPR) is the key result for each steady-state RETRAN/TCPYA01 analysis. These results allow for the development of functional relationships, describing AP as a function of ICPR, and AF and BPF as functions of AP for each fuel type. These relationships are used in the iterative process used during the transient calculations as described below and shown in Figure 7.1.1.

The second part iterates on the hot channel initial power level. This is necessary because the ΔCPR for a given transient varies with Initial Critical Power Ratio (ICPR). However, only the ΔCPR corresponding to a transient MCPR equal to the FCISL limit (i.e., 1.07 + ΔCPR = ICPR) is appropriate. The approximate constancy of the ΔCPR/ICPR ratio is useful in these iterations. Each iteration requires a RETRAN hot channel run to calculate the transient enthalpies, flows, pressure and saturation properties at each time step. These are required for input to the TCPYA01 code. TCYPA01 is then used to calculate a CPR at each time step during the transient, from which a transient ΔCPR is derived. The hot channel model assumes a chopped cosine axial power shape with a peak/average ratio of 1.4.

As noted in Section 6.1, analyses for the Reload Cycle included benchmarking the FIBWR model against vendor-supplied thermal-hydraulic information. Therefore, the FIBWR results of AF and BPF for a given AP and core pressure drop are passed directly to RETRAN. As shown in Figure 7.1.1, the current iterative process involves a single loop.

7.1.2 Initial Conditions and Assumptions

The initial conditions for the system simulations are based on maximum turbine capacity of 105% of rated steam flow. The corresponding reactor conditions are 104.5% core thermal power and 100% core flow. The core axial power distribution for each of the exposure points is based on the 3-dimensional SIMULATE-3 [3-4] predictions associated with the generation of the reactivity data (Section 7.1.3). The core inlet enthalpy is set so that the amount of carryunder from the steam separators and the quality in the liquid region outside the separators is as close to zero as possible. For fast pressurization transients, this maximizes the initial pressurization rate and predicts a more severe neutron power spike. A summary of the initial operating state used for the system simulations is provided in Table 7.1.1.

Vermont Yankee operators adjust core flow during the cycle for short-term maneuvering. During this type of operation, core flow may be as low as 87% while at 100% power. To ensure the safety analysis bounds these conditions, transients are reanalyzed at the limiting exposure statepoint (limiting in terms of an increase in ΔCPR) corresponding to these conditions. These analyses are performed at both the "Measured" and the "67B" scram times. The ΔCPR penalty (defined as the difference in ΔCPR) generated during this reanalysis is applied to the applicable transient ΔCPR results.

Assumptions specific to a particular transient are discussed in the section describing the transient. In general, the following assumptions are made for all transients:

1. Scram setpoints are at Technical Specification [7] limits.

2. Protective system logic delays are at equipment specification limits.

3. Safety/relief valve and safety valve capacities are based on Technical Specification rated values.

4. Safety/relief valve and safety valve setpoints are modeled as being at the Technical Specification upper limit. Valve responses are based on slowest specified response values.

5. Control rod drive scram speed is based on the Technical Specification limits. The analysis addresses a dual set of scram speeds, referred to as the "Measured" and the "67B" scram times. "Measured" refers to the faster scram times given in Section 3.3.C.1.1 of the Technical Specifications. "67B" refers to the slower scram times given in Section 3.3.C.1.2 of the Technical Specifications.

7.1.3 One-Dimensional Cross Sections and Kinetics Parameters

The methods used to generate the one-dimensional (1-D) cross sections and kinetics parameters as a function of fuel temperature, moderator density, moderator temperature, and scram are described in detail in Reference 19. The method is outlined below.

A complete set of 1-D cross sections, 1-D kinetics parameters, the axial power distribution, and the kinetics parameters are generated from base states established for EOFPL, EOFPL-1000 MWD/ST, EOFPL-2000 MWD/ST, and BOC exposure statepoints. These statepoints are characterized by exposure and void history distributions, control rod patterns, and core thermal-hydraulic conditions. The latter are consistent with the assumed system transient conditions provided in Table 7.1.1.

The BOC base state is established by shuffling from the previously defined Current Cycle endpoint into the Reload Cycle loading pattern. A criticality search provides an estimate of the BOC critical rod pattern. The EOFPL and intermediate core exposure and void history distributions are calculated with a Haling depletion as described in Section 5.2. The EOFPL state is unrodded. As such, it is defined sufficiently. However, the EOFPL-1000 MWD/ST and EOFPL-2000 MWD/ST exposure statepoints require base control rod patterns. These are developed to be as "black and white" as

possible. That is, beginning with the rodded depletion configuration, all control rods which are more than half inserted are fully inserted, and all control rods which are less than half inserted are fully withdrawn. If the SIMULATE-3 [3-4] calculated parameters are within operating limits, then this configuration becomes the base case. If the limits are exceeded, a minimum number of control rods are adjusted a minimum number of notches until the parameters fall within limits. Using this method, the control rod patterns and resultant power distributions minimize the scram reactivity and maximize the core average moderator density reactivity coefficient. For the events analyzed, this tends to maximize the transient power response.

At each exposure statepoint, a SIMULATE-3 initial control state reference case is run. A series of perturbation cases are run with SIMULATE-3 to independently vary the fuel temperature, moderator temperature, and core pressure. All other variables normally associated with the SIMULATE-3 cross sections are held constant at the reference state. To obtain the effect of the control rod scram, another SIMULATE-3 reference case is run with all-rods-in. The perturbation cases described above are run again from this reference case. For each control state, a data set of kinetics parameters and cross sections is generated as a function of the perturbed variable. There is a table set for each of the 27 neutronic regions, 25 regions to represent the active core and one region each for the bottom and top reflectors. Figures 7.2.1 through 7.2.6 show the transient response of scram reactivity in the "Measured" scram time analyses.

7.1.4 Transients Analyzed

Past licensing analysis has shown that the transients which result in the minimum core thermal margins are:

1. Generator load rejection with complete failure of the turbine bypass system.

2. Turbine trip with complete failure of the turbine bypass system.

3. Loss of feedwater heating.

The "feedwater controller failure" (maximum demand) transient is not a limiting transient for Vermont Yankee, because of the plant's 110% steam flow bypass system. Past analyses have shown this transient to be considerably less limiting than any of the above for all exposure points. The events reported herein are limiting; no other transients would produce more restrictive MCPR operating limits for the Reload Cycle. Brief descriptions and the results of the transients analyzed are provided in the following section.

7.2 Transient Analysis Results

The transients selected for consideration were analyzed at exposure points of EOFPL, EOFPL-1000 MWD/ST, and EOFPL-2000 MWD/ST; the loss of feedwater heating transient was also evaluated at BOC conditions. The transient results reported in Table 7.2.1 correspond to the limiting bundle type in the core. The MCPR limits in Table 7.2.1 are calculated by adding the calculated ΔCPR to the FCISL.

7.2.1 Turbine Trip Without Bypass Transient (TTWOBP)

The transient is initiated by a rapid closure (0.1 second closing time) of the turbine stop valves. It is assumed that the steam bypass valves, which normally open to relieve pressure, remain closed. A reactor protection system signal is generated by the turbine stop valve closure switches. Control rod drive motion is conservatively assumed to occur 0.27 seconds after the start of turbine stop valve motion. The ATWS recirculation pump trip is assumed to occur at a setpoint of 1150 psig dome pressure. A pump trip time delay of 1.0 second is assumed to account for logic delay and M-G set generator field collapse. In simulating the transient, the bypass piping volume up to the valve chest is lumped into the control volume upstream of the turbine stop valves. Predictions of the salient system parameters at the three exposure points are shown in Figures 7.2.1 through 7.2.3 for the "Measured" scram time analysis.

7.2.2 Generator Load Rejection Without Bypass Transient (GLRWOBP)

The transient is initiated by a rapid closure (0.3 seconds closing time) of the turbine control valves. As in the case of the turbine trip transient, the bypass valves are assumed to fail. A reactor protection system signal is generated by the hydraulic fluid pressure switches in the acceleration relay of the turbine control system. Control rod drive motion is conservatively assumed to occur 0.28 seconds after the start of turbine control valve motion. The same modeling regarding the ATWS pump trip and bypass piping is used as in the turbine trip simulation. The influence of the accelerating main turbine generator on the recirculation system is simulated by specifying the main turbine generator electrical frequency as a function of time for the M-G set drive motors. The main turbine generator frequency curve is based on a 100% power plant startup test and is considered representative for the simulation. The system model predictions for the three exposure points are shown in Figures 7.2.4 through 7.2.6 for the "Measured" scram time analysis.

7.2.3 Loss of Feedwater Heating Transient (LOFWH)

A feedwater heater can be lost in such a way that the steam extraction line to the heater is shut off or the feedwater flow bypasses one of the heaters. In either case, the reactor will receive cooler feedwater, which will produce an increase in the core inlet subcooling, resulting in a reactor power increase.

The response of the system due to the loss of 100°F of the feedwater heating capability was analyzed. This represents the maximum expected feedwater temperature reduction for a single heater or group of heaters that can be tripped or bypassed by a single event.

Vermont Yankee has a scram setpoint of 120% of rated power as part of the Reactor Protection System (RPS) on high neutron flux. In this analysis, no credit was taken for scram on high neutron flux, thereby allowing the

reactor power to reach its peak without scram. This approach was selected to provide a bounding and conservative analysis for events initiated from any power level.

The transient response of the system was evaluated at several exposures during the cycle. The transient evaluation at EOFPL-1000 MWD/ST was found to be the limiting case between BOC to EOFPL. The results of the system response to a loss of 100°F feedwater heating capability evaluated at EOFPL-1000 MWd/ST as predicted by the RETRAN code are presented in Figure 7.2.7.

7.3 Overpressurization Analysis Results

Compliance with ASME vessel code limits is demonstrated by an analysis of the Main Steam Isolation Valves (MSIV) closing with failure of the MSIV position switch scram. EOFPL conditions were analyzed. The system model used is the same as that used for the transient analysis (Section 7.1.1). The initial conditions and modeling assumptions discussed in Section 7.1.2 are applicable to this simulation.

The transient is initiated by a simultaneous closure of all four MSIVs. A 3.0 second closing time, which is the Technical Specification minimum, is assumed. A reactor scram signal is generated on APRM high flux. Control rod drive motion is conservatively assumed to occur 0.28 seconds after reaching the high flux setpoint. The system response is shown in Figure 7.3.1 for the "Measured" scram time analysis.

The maximum pressures at the bottom of the reactor vessel calculated for the "Measured" scram time analysis and for the "67B" scram time analysis are given in Table 7.3.1. These results are within the allowable code limit of 10% above vessel design pressure for upset conditions, or 1375 psig.

7.4 Local Rod Withdrawal Error Transient Results

The rod withdrawal error (RWE) is a local core transient caused by an operator erroneously withdrawing a control rod in the continuous withdrawal mode. If the core is operating at its operating limits for MCPR and LHGR at the time of the error, then withdrawal of a control rod could increase both local and core power levels with the potential for overheating the fuel.

There is a broad spectrum of core conditions and control rod patterns which could be present at the time of such an error. For most normal situations it would be possible to fully withdraw a control rod without exceeding 1% clad plastic strain or violating the FCISL.

To bound the most severe of postulated rod withdrawal error events, a portion of the core MCPR operating limit envelope is specifically defined such that the cladding limits are not violated. The consequences of the error depend on the local power increase, the initial MCPR of the neighboring locations and the ability of the Rod Block Monitor (RBM) System to stop the withdrawing rod before MCPR reaches the FCISL.

The most severe transient postulated begins with the core operating according to normal procedures and within normal operating limits. The operator makes a procedural error and attempts to fully withdraw the maximum worth control rod at maximum withdrawal speed. The core limiting locations are close to the error rod. They experience the spatial power shape transient as well as the overall core power increase.

The core conditions and control rod pattern are conservatively modeled for the bounding case by specifying the following set of concurrent worst case assumptions:

1. The rod should have high reactivity worth. This is provided for by analysis of the core at several exposure points around the core peak reactivity. The test patterns are developed with xenon-free conditions. The xenon-free condition and the additional control

rod inventory needed to maintain criticality exaggerates the worth of the withdrawn control rod when compared to normal operation with normal xenon levels.

2. The core is initially at 104.5% power and 100% flow.

3. The core power distribution is adjusted with the available control rods to place the locations within the four by four array of bundles around the error rod as close to the operating limits as possible.

4. Of the many patterns tested, the pattern with the highest ΔCPR results is selected as the bounding case.

The RBM System's ability to terminate the bounding case is evaluated on the following bases:

1. Technical Specifications allow each of the separate RBM channels to remain operable if at least half of the Local Power Range Monitor (LPRM) inputs at every level are operable. For the interior RBM channels tested in this analysis, there are a maximum of four LPRM inputs per level. One RBM channel averages the inputs from the A and C levels; the other channel averages the inputs from the B and D levels. Considering the inputs for a single channel, there are eleven failure combinations of none, one and two failed LPRM strings. The RBM channel responses are evaluated separately at these eleven input failure conditions. Then, for each channel taken separately, the lowest response as a function of error rod position is chosen for comparison to the RBM setpoint.

2. The event is analyzed separately in each of the four quadrants of the core due to the differing LPRM string physical locations relative to the error rod.

Technical Specifications require that both RBM channels be operable during normal operation. Thus, the first channel calculated to intercept the RBM setpoint is assumed to stop the rod. To allow for control system delay times, the rod is assumed to move two inches after the intercept and stop at the following notch.

The analysis is performed using SIMULATE-3 [3-4]. Two separate cases are presented from numerous explicit SIMULATE analyses. The reactor conditions and case descriptions are shown in Figures 7.4.1 and 7.4.2. Case 1 analyzes the bounding event with zero xenon at the most reactive point in the cycle for the worst case abnormal rod pattern configuration. Case 2 is the worst of the 104.5% power conditions modeled with more normal control rod patterns and equilibrium xenon. The transient results, the ΔCPR and maximum linear heat generation rate (MLHGR) values, are also shown in Figures 7.4.1 and 7.4.2. The ΔCPR values are evaluated such that the implied MCPR operating limit equals FCISL + ΔCPR. This is done by conserving the figure of merit (ΔCPR/ICPR) shown by the SIMULATE calculations. The use of this method provides valid ΔCPR values in the analysis of normal operating states where locations near the assumed error rod are not initially near the MCPR operating limit.

Case 2 is the worst of all the rod withdrawal transients analyzed from 104.5% power, full flow and normal rod pattern conditions. Case 2 is bounded by Case 1 with substantial MCPR margin. The Case 1 RBM channel responses are shown in Figures 7.4.3 and 7.4.4. They also show the control rod position at the point where the weakest RBM channel response first intercepts the RBM setpoint. For this same bounding case, the operating limit ΔCPR envelope component versus RBM setpoint is taken from Figure 7.4.1. The same figure shows the resultant LHGR assuming the limiting bundle is placed on the operating limit of 14.4 kW/ft prior to the withdrawal. The calculation includes the 2.2% power spiking penalty. The limiting bundle MLHGR demonstrates margin to the 1% plastic strain limit given the low exposure of the limiting bundle. High exposure bundles which have low 1% plastic strain limits are never limiting.

7.5 Misloaded Bundle Error Analysis Results

7.5.1 Rotated Bundle Error

The primary result of a bundle rotation is a large increase in local pin peaking and R-factor as higher enrichment pins are placed adjacent to the surrounding wide water gaps. In addition, there may be a small increase in reactivity, depending on the exposure and void fraction states. The R-factor increase results in a CPR reduction, while the local pin peaking factor increase results in a higher pin LHGR. The objective of the analysis is to ensure that, in the worst possible rotation, the LHGR and CPR safety limits are not violated with the most limiting monitored bundles on their operating limits.

To analyze the CPR response, rotated bundle R-factors as a function of exposure are developed by adding the largest possible ΔR-factor resulting from a rotation to the exposure dependent R-factors of the properly oriented bundles [12]. Using these rotated bundle R-factors, the MCPR values resulting from a bundle rotation are determined using SIMULATE. This is done for each control rod sequence throughout the cycle. The process is repeated with the K-infinity of the limiting bundle modified slightly to account for the increase in reactivity resulting from the rotation. For each sequence, the MCPR for the properly oriented bundles is adjusted by a ratio necessary to place the corresponding rotated CPR on its FCISL. The maximum of these adjusted MCPRs is the rotated bundle operating limit.

To determine the MLHGR resulting from a rotation, the ratios of the maximum rotated bundle local peaking factor to the maximum properly oriented bundle local peaking are determined for the expected range of exposure and void conditions. The maximum of this ratio is applied to the LHGR operating limits of 13.4 kW/ft and 14.4 kW/ft. This maximum rotated bundle LHGR is, in addition, modified to account for the possible reactivity increase resulting from the rotation. It is also increased by the 2.2% power spiking penalty.

The results of the rotated bundle analysis are given in Table 7.5.1. Comparing Table 7.5.1 to Table 4.2.2, there is sufficient margin to the 1% plastic strain limit.

7.5.2 Mislocated Bundle Error

Misloading a high reactivity assembly into a region of high neutron importance results in a location of high relative assembly average power. Since the assembly is assumed to be properly oriented (not rotated), R-factors used for the misloaded bundle are the standard values for the fuel type.

The analysis uses multiple SIMULATE-3 cases to examine the effects of explicitly mislocating every older interior assembly in a quarter core with a fresh or once-burned assembly. Because of symmetry, the results apply to the whole core. Edge bundles are not examined because they are never limiting, due to neutron leakage.

The effect of the successive mislocations is examined for every control rod sequence throughout the cycle. For each sequence, the MCPR for the properly loaded core is compared to the MCPR of the misloaded core at the misloaded location. The MCPR for the properly loaded core is adjusted by a ratio necessary to place the mislocated assembly on the FCISL. The maximum of these adjusted MCPRs is the mislocated bundle operating limit.

The results of the mislocated bundle analysis are given in Table 7.5.2. Comparing Table 7.5.2 to Table 4.2.2, there is sufficient margin to the 1% plastic strain limit.

7.6 Control Rod Drop Accident Results

The control rod sequences are a series of rod withdrawal and banked withdrawal instructions specifically designed to minimize the worths of individual control rods. The sequences are examined so that, in the event of the uncoupling and subsequent free fall of the rod, the incremental rod worth is acceptable. Incremental rod worth refers to the fact that rods beyond

Group 2 are banked out of the core and can only fall the increment from full-in to the rod drive withdrawal position. Acceptable worth is one which produces a maximum fuel enthalpy less than 280 calories/gram.

Some out-of-sequence control rods could accrue potentially high worths. However, the Rod Worth Minimizer (RWM) will prevent withdrawing an out-of-sequence rod, if accidentally selected. The RWM is functionally tested before each startup.

The sequence in the RWM will take the plant from All Rods In (ARI) to well above 20% core thermal power. Above 20% power even multiple operator errors will not create a potential rod drop situation above 280 calories per gram [20-22]. Below 20% power, however, the sequences must be examined for incremental rod worth. This is done throughout the cycle using the full core, xenon-free SIMULATE-3 model.

Both the A and B sequences were examined at various exposures throughout the cycle. For startup, the rods are grouped, as shown in Figures 7.6.1 and 7.6.2, and are pulled in numerical order. All the rods in one group are pulled out before the pulling of the next group begins. The rods in the first two groups are individually pulled from full-in to full-out. Beyond Group 2, the rods are banked out using procedures [23-24] which reduce the rod incremental worths.

The potentially high worths that occur in the pulling of the Group 1 rods are ignored because the reactor is subcritical in Group 1. Therefore, if a rod drops from any configuration in the first group, its excess reactivity contribution to the Rod Drop Accident (RDA) is zero. Successive reloads of axially zoned fuel have extended this subcriticality situation to the second group as well.

The second group of rods was examined using the analysis procedure described in Reference 25. Relatively few control rod configurations were found to be critical. For conservatism, "critical" was defined as the

SIMULATE-3 average cold critical K_{eff} minus 1% ΔK (reactivity anomaly criteria). The few potentially critical configurations in Group 2 contributed less excess reactivity to the RDA than subsequent configurations in Group 3.

Most pre-drop cases in Group 3 are critical. Therefore, the entire dropped rod worth contributes toward the RDA excess reactivity insertion. The method used to evaluate Group 3 involved pulling Groups 1 and 2 out and banking Group 3 to varying positions. The types of cases examined included:

1. Banked positions 04, 08, 12, and 48 (full-out).

2. Group 3 rods pulled out of sequence, creating high flux regions.

3. Xenon-free conditions, both cold moderator and "standby" (i.e., 1020 psia).

4. Group 3 rods dropping from 00 (full-in) to the appropriate banked position.

5. Stuck rods from previously pulled Group 1 or 2 dropping from 00 to 48.

The highest worth results, presented in Table 7.6.2, fit under the bounding analysis in References 20 through 22.

7.7 Refueling Accident Results

If any assembly is damaged during refueling, then a fraction of the fission product inventory could be released to the environment. The source term for the refueling accident is the maximum gap activity within any bundle. The source term includes contributions from both noble gases and iodines. The calculation of maximum gap activity is based on the MAPLHGRs, the maximum operating fuel centerline temperatures, and maximum bundle burnup.

The fuel rod gap activity for the Reload Cycle is bounded by the values used in Section 14.9 of the FSAR, Reference 26.

TABLE 7.1.1

VY CYCLE 15 SUMMARY OF SYSTEM TRANSIENT MODEL
INITIAL CONDITIONS FOR TRANSIENT ANALYSES

Core Thermal Power (MWth)	1664.0
Turbine Steam Flow (% NBR)	105
Total Core Flow (10^6lbm/hr)	48.0
Core Bypass Flow (10^6lbm/hr)*	5.8
Core Inlet Enthalpy (BTU/lbm)	521.6
Steam Dome Pressure (psia)	1034.7
Turbine Inlet Pressure (psia)	986.0
Total Recirculation Flow (10^6lbm/hr)	23.4
Core Plate Differential Pressure (psi)	19.7
Narrow Range Water Level (in.)	162
Average Fuel Gap Conductance	(See Section 4.2)

* Includes water rod flow.

TABLE 7.2.1

VY CYCLE 15 TRANSIENT ANALYSIS RESULTS

Transient	Exposure	Peak Prompt Power (Fraction of Initial Value)	Peak Avg. Heat Flux (Fraction of Initial Value)	ΔCPR	Operating MCPR Limits
Turbine Trip Without Bypass, "Measured" Scram Time	EOFPL	3.347	1.244	.18	1.25
	EOFPL-1000	2.453	1.155	.11	1.18
	EOFPL-2000	1.712	1.060	.04	1.11
Turbine Trip Without Bypass, "67B" Scram Time	EOFPL	3.847	1.285	.22	1.29
	EOFPL-1000	2.834	1.206	.15	1.22
	EOFPL-2000	2.114	1.121	.08	1.15
Generator Load Rejection Without Bypass, "Measured" Scram Time	EOFPL	3.240	1.228	.16	1.23
	EOFPL-1000	2.428	1.143	.10	1.17
	EOFPL-2000	1.677	1.040	.02	1.09
Generator Load Rejection Without Bypass, "67B" Scram Time	EOFPL	3.704	1.284	.20	1.27
	EOFPL-1000	2.990	1.208	.15	1.22
	EOFPL-2000	2.297	1.117	.07	1.14
Loss of 100°F Feedwater Heating	EOFPL	1.147	1.148	.11	1.18
	EOFPL-1000	1.256	1.163	.13	1.20
	EOFPL-2000	1.242	1.151	.12	1.19
	BOC	1.152	1.152	.12	1.19

TABLE 7.3.1

VY CYCLE 15 OVERPRESSURIZATION ANALYSIS RESULTS

Conditions	Maximum Pressure at Reactor Vessel Bottom (psia)
"Measured" Scram Time	1262
"67B" Scram Time	1293

TABLE 7.5.1

VY CYCLE 15 ROTATED BUNDLE ANALYSIS RESULTS

Operating MCPR Limit	Maximum Attainable LHGR (kW/ft)
1.23	19.95

TABLE 7.5.2

VY CYCLE 15 MISLOCATED BUNDLE ANALYSIS RESULTS

Operating MCPR Limit	Maximum Attainable LHGR (kW/ft)
1.20	19.85

TABLE 7.6.2

VY CYCLE 15 CONTROL ROD DROP ANALYSIS RESULTS

Maximum Incremental Rod Worth Calculated Cold, Xenon-Free	0.67% ΔK
Bounding Analysis Worth for Enthalpy Less than 280 Calories per Gram [20-22]	1.30% ΔK

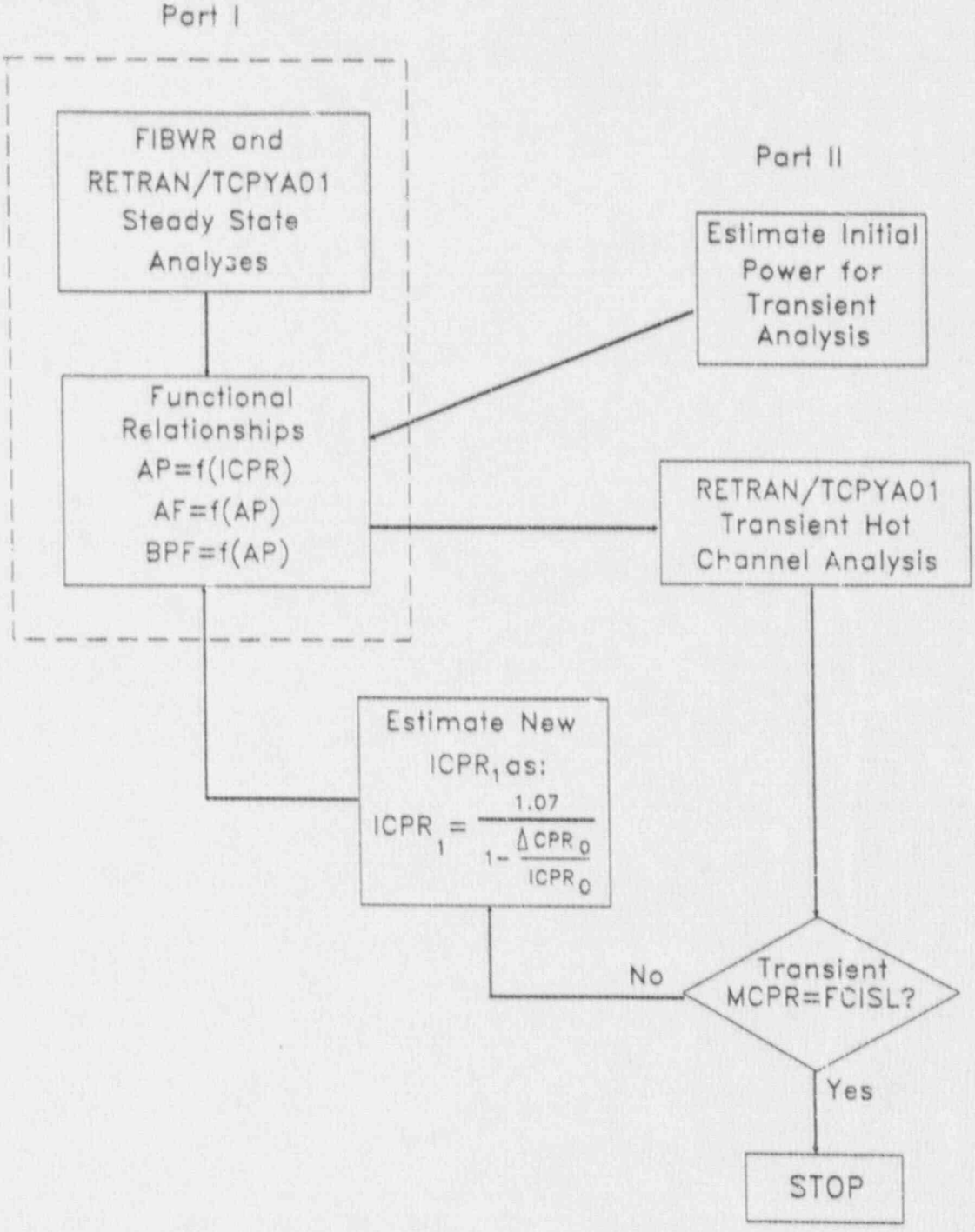

FIGURE 7.1.1

Flow Chart for the Calculation of ΔCPR Using the RETRAN/TCPYA01 Codes

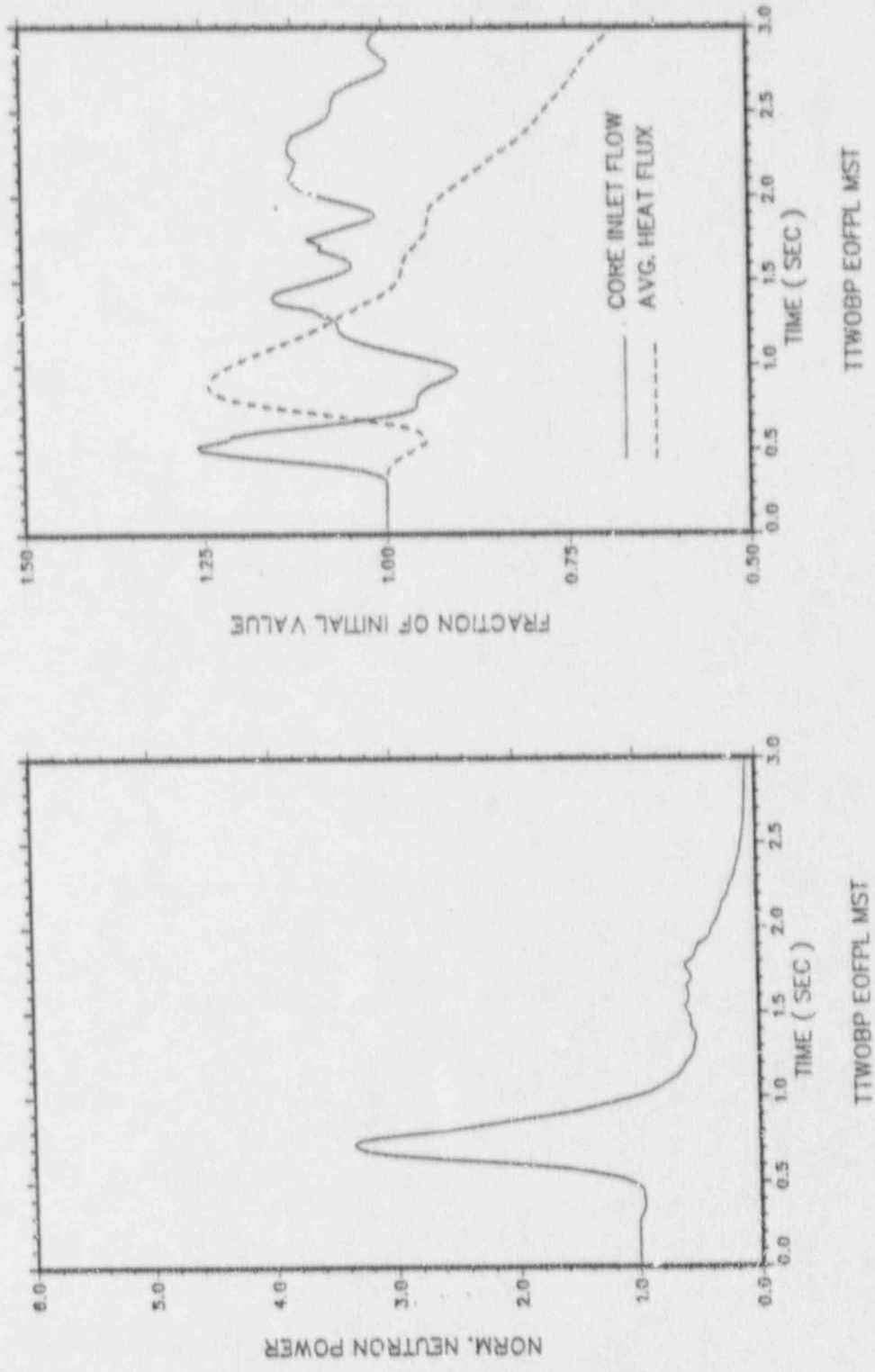

FIGURE 7.2.1-1

Turbine Trip Without Bypass, EOFPL15
Transient Response Versus Time, "Measured" Scram Time

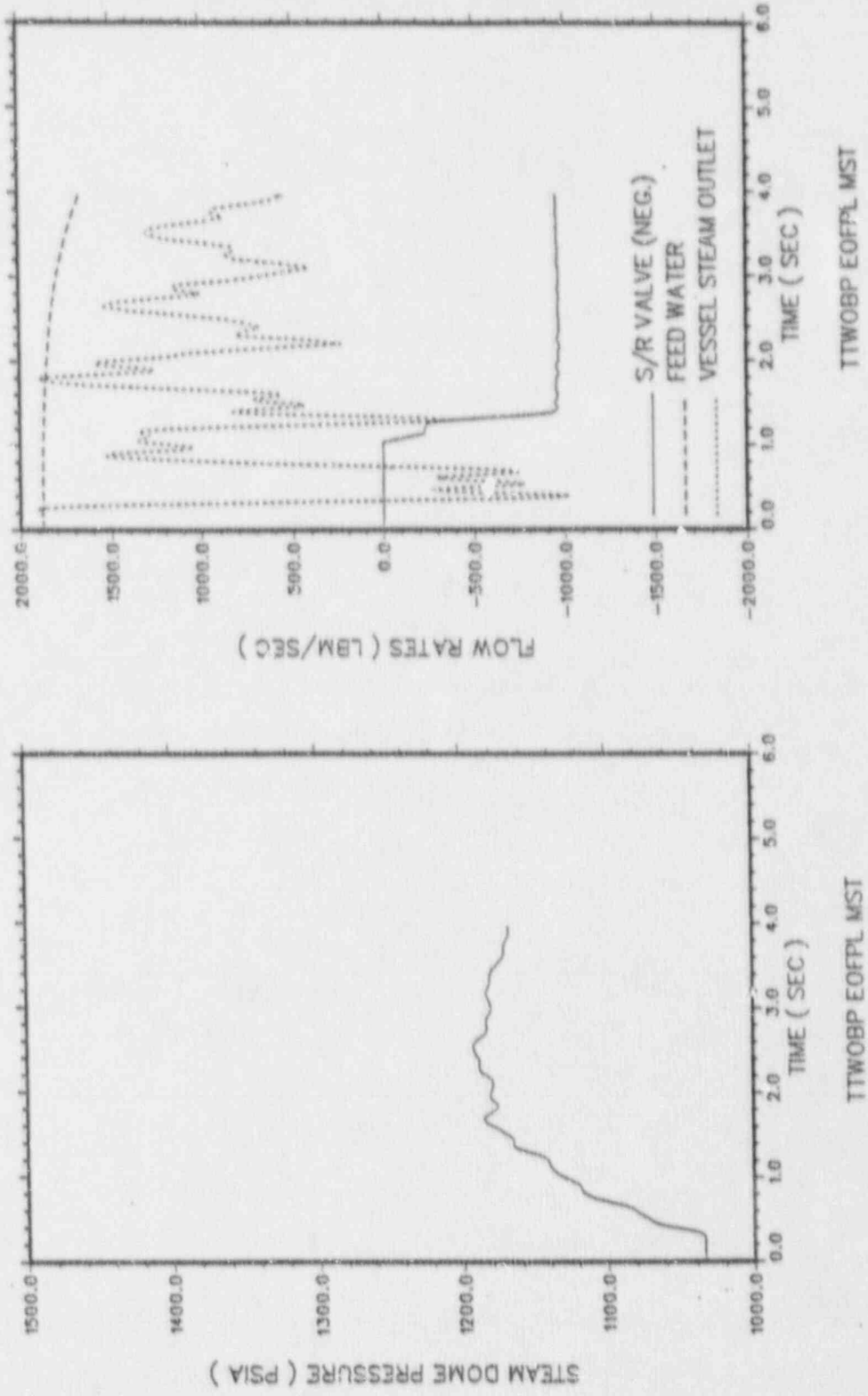

FIGURE 7.2.1-2

Turbine Trip Without Bypass, EOFPL15
Transient Response Versus Time, "Measured" Scram Time

PP40/10

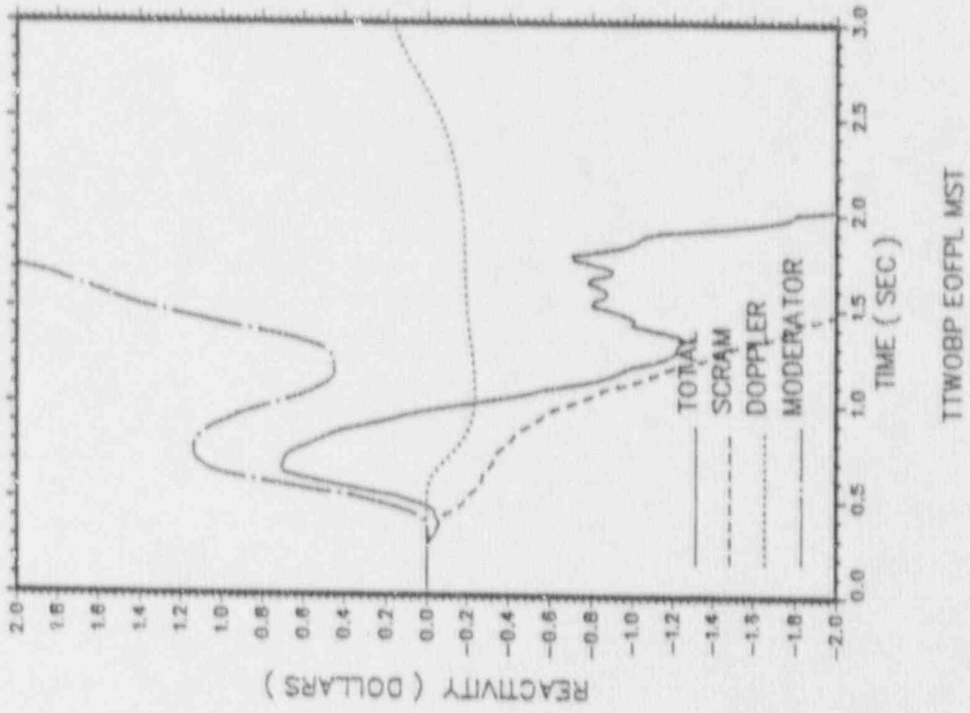

FIGURE 7.2.1-3

Turbine Trip Without Bypass, EOFPL15
Transient Response Versus Time, "Measured" Scram Time

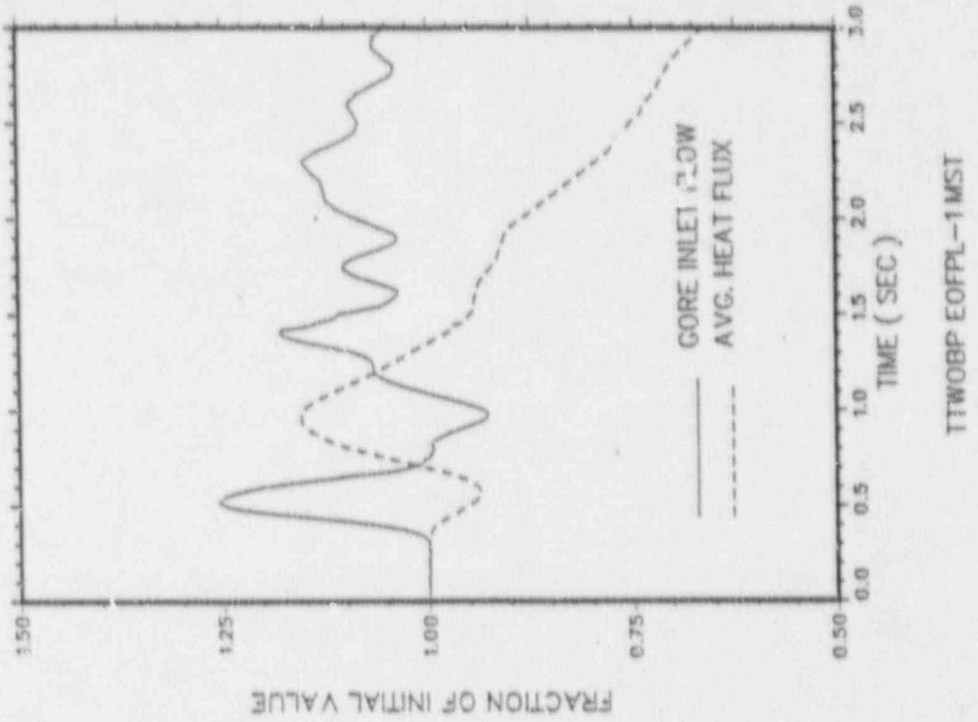

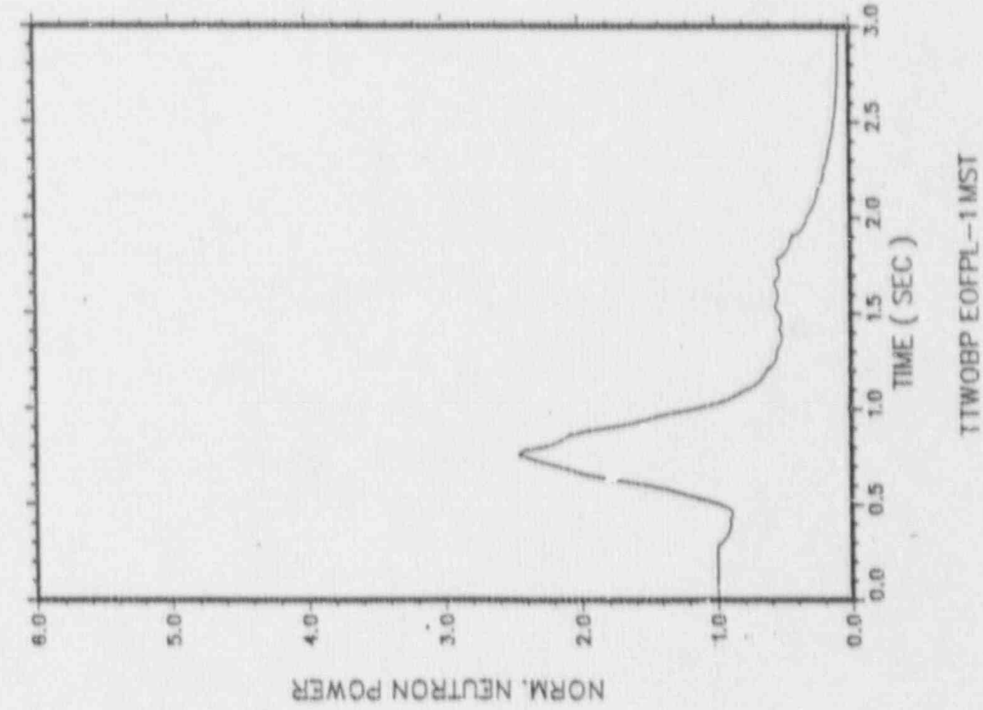

FIGURE 7.2.2-1

Turbine Trip Without Bypass, EOFPL15-1000 MWD/ST
Transient Response Versus Time, "Measured" Scram Time

WPP40/10

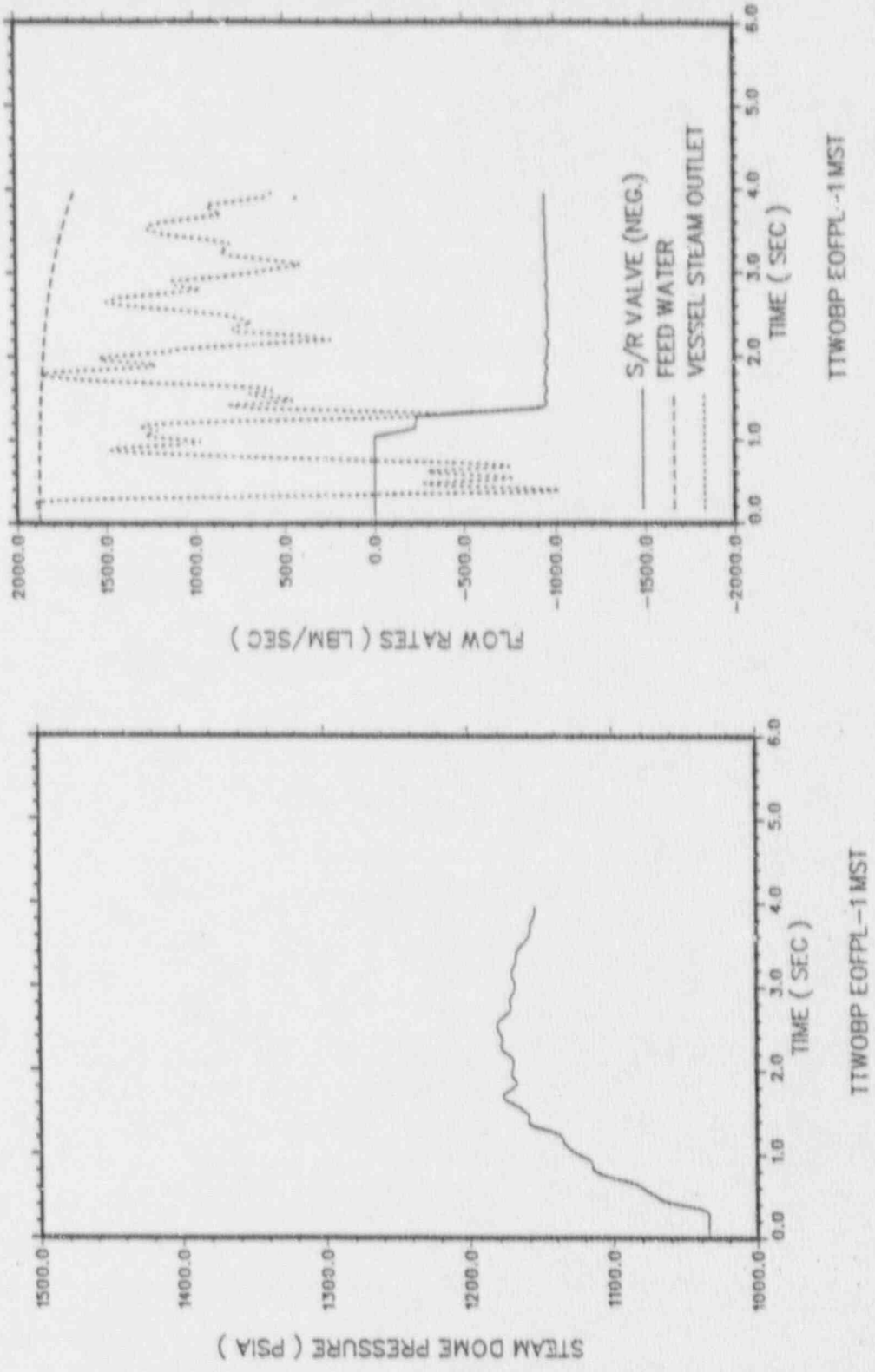

FIGURE 7.2.2-2

Turbine Trip Without Bypass, EOFPL15-1000 MWD/ST
Transient Response Versus Time, "Measured" Scram Time

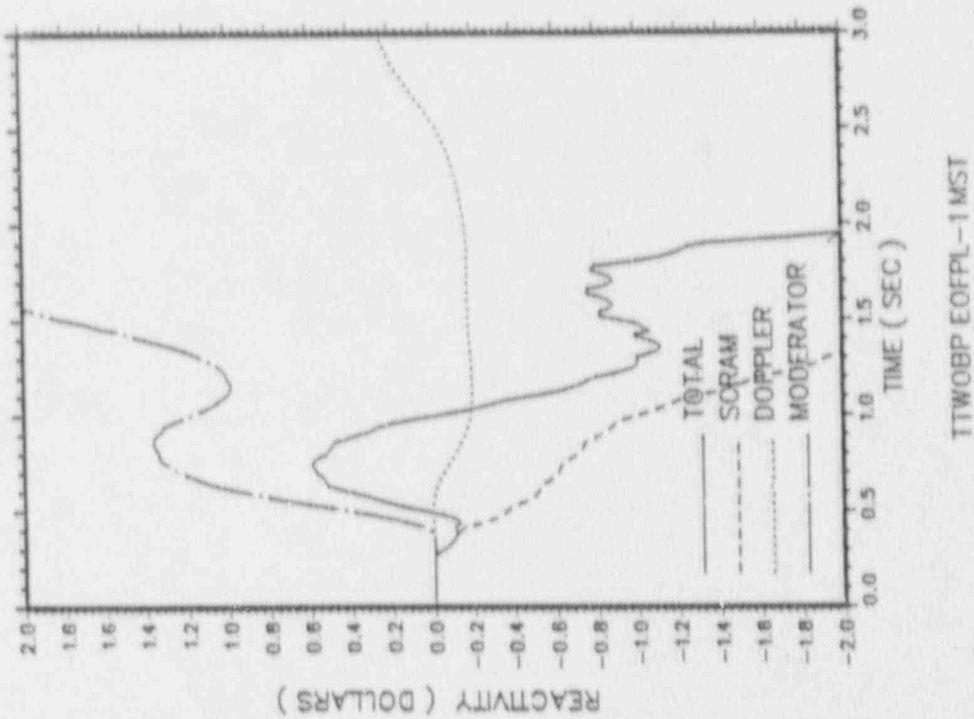

FIGURE 7.2.2-3

Turbine Trip Without Bypass, EOFPL15-1000 MWD/ST
Transient Response Versus Time, "Measured" Scram Time

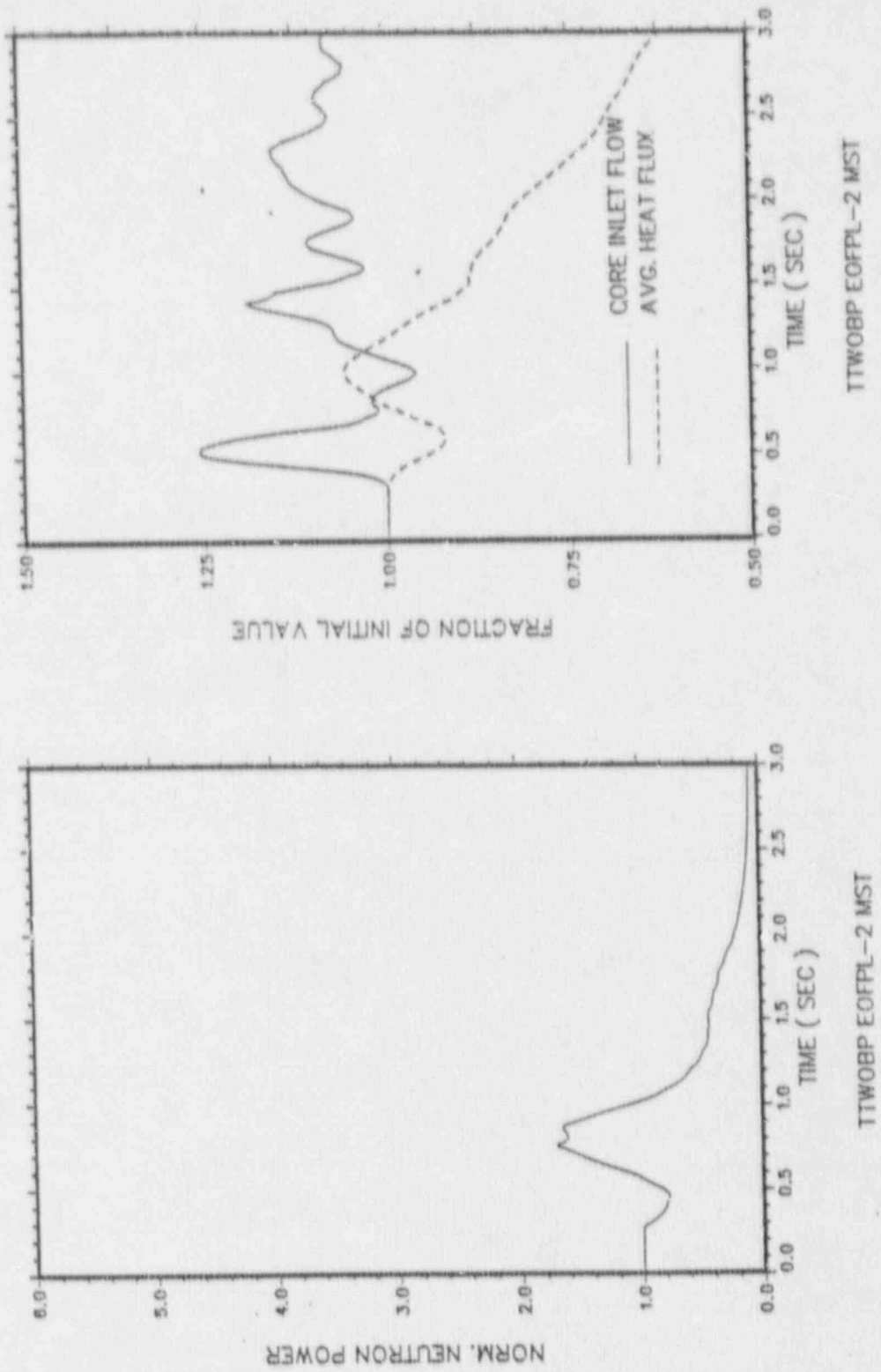

FIGURE 7.2.3-1

Turbine Trip Without Bypass, EOFPL-2000 MWD/ST
Transient Response Versus Time, "Measured" Scram Time

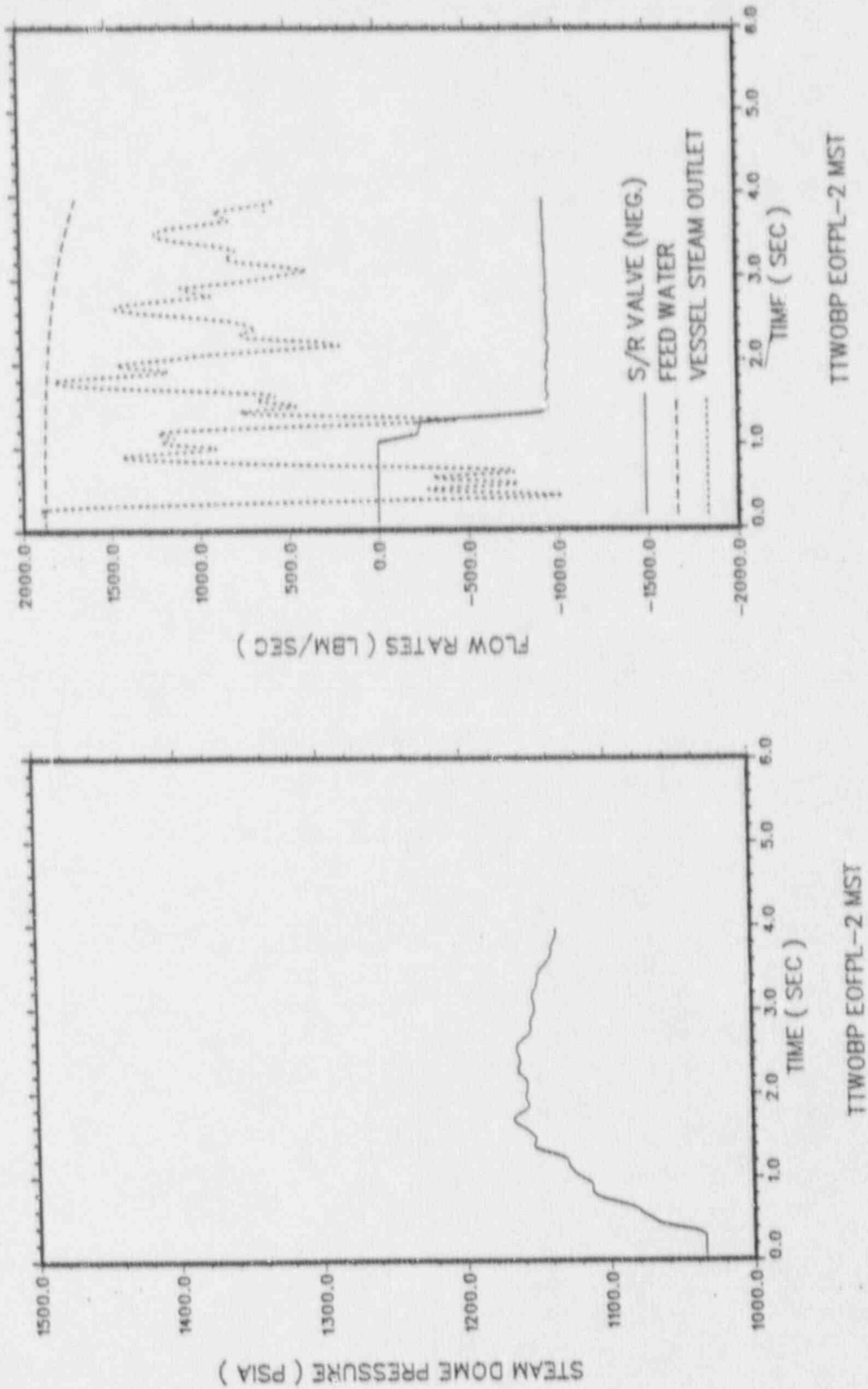

FIGURE 7.2.3-2

Turbine Trip Without Bypass, EOFPL-2000 MWD/ST
Transient Response Versus Time, "Measured" Scram Time

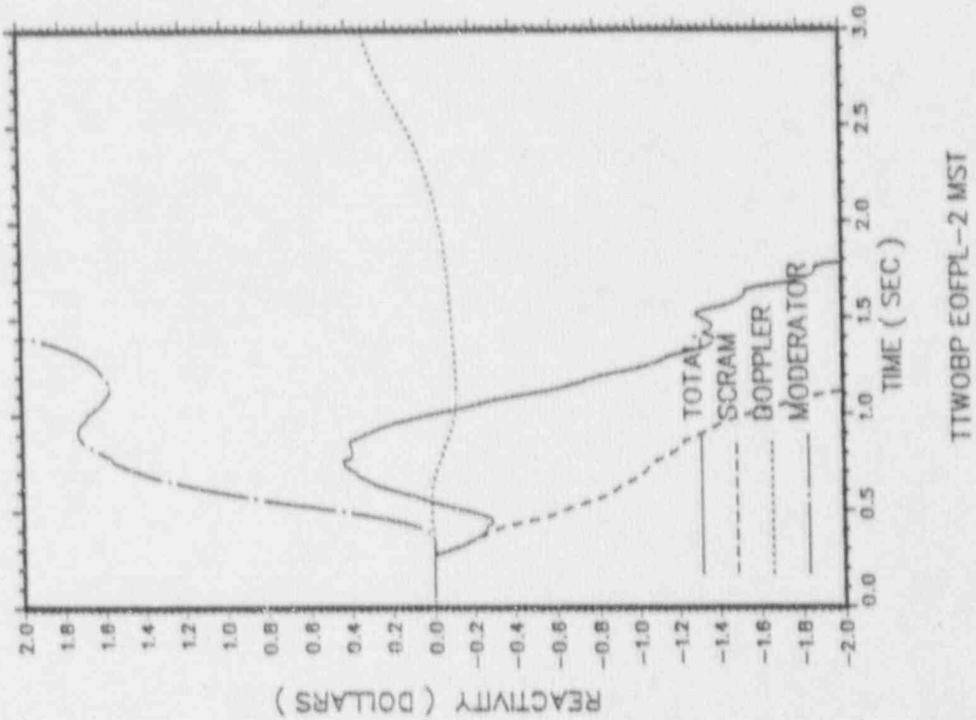

FIGURE 7.2.3-3

Turbine Trip Without Bypass, EOFPL-2000 MWD/ST
Transient Response Versus Time, "Measured" Scram Time

WPP40/10

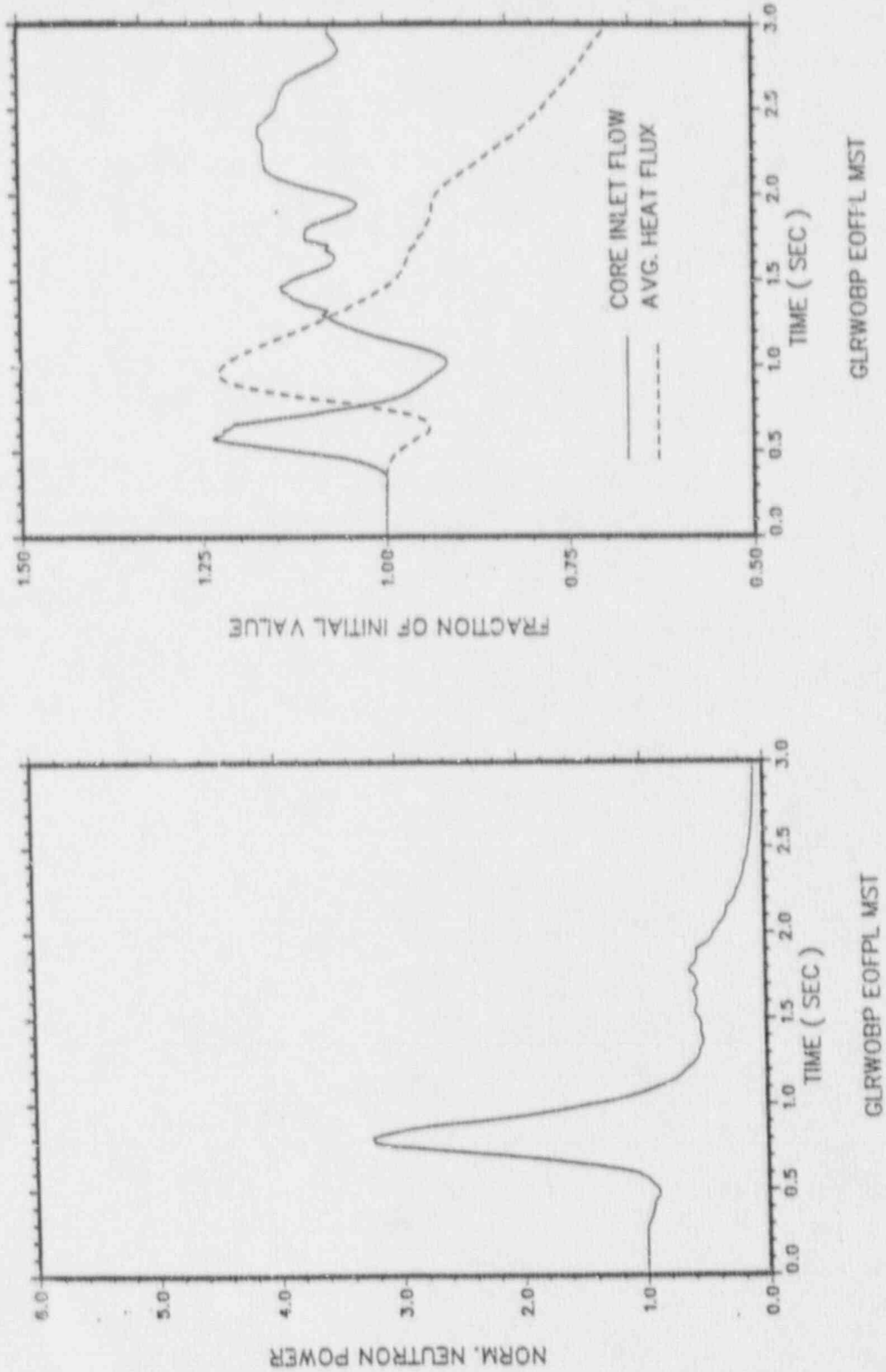

FIGURE 7.2.4-1

Generator Load Rejection Without Bypass, EOFPL15
Transient Response Versus Time, "Measured" Scram Time

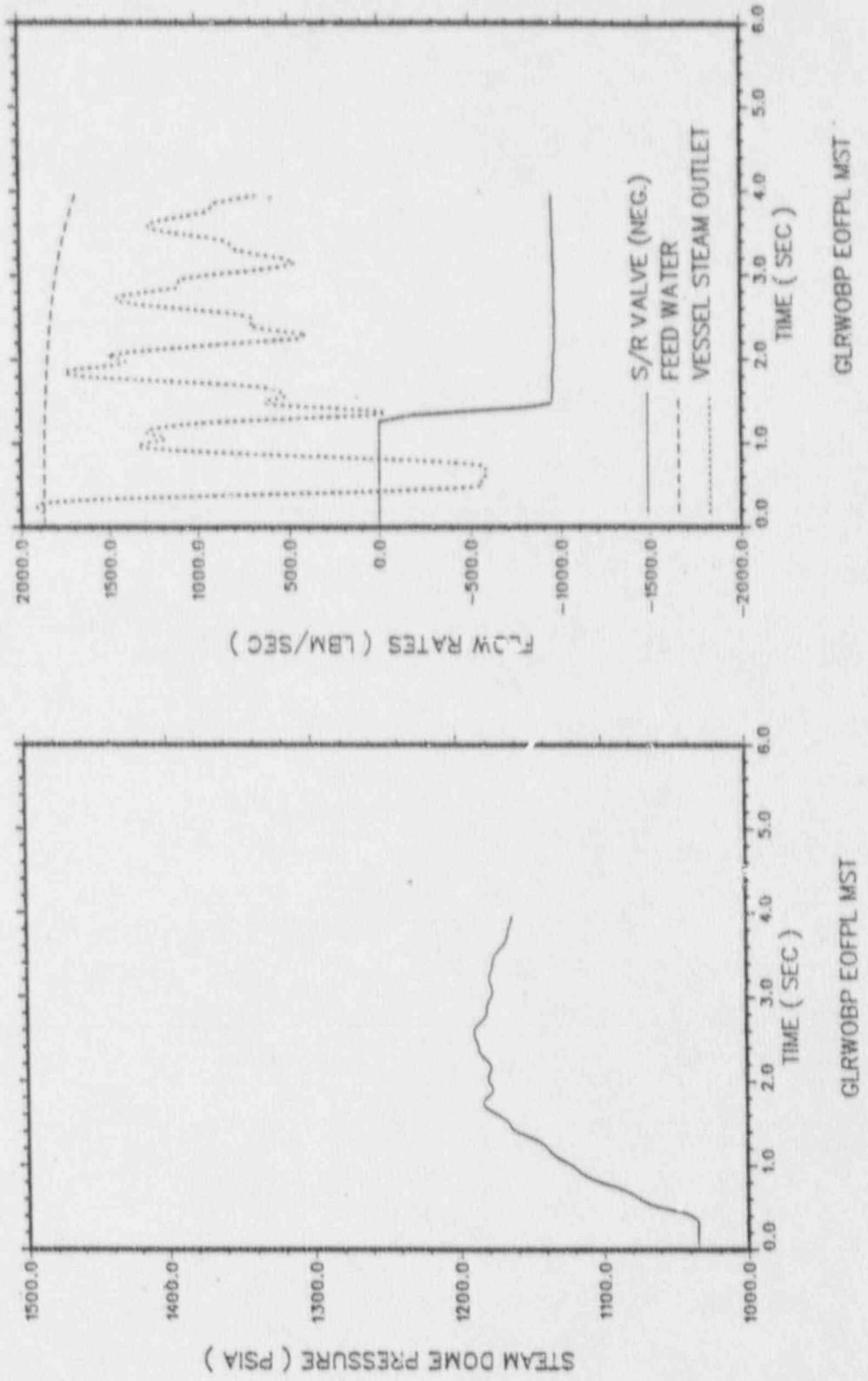

FIGURE 7.2.4-2

Generator Load Rejection Without Bypass, EOFPL15
Transient Response Versus Time, "Measured" Scram Time

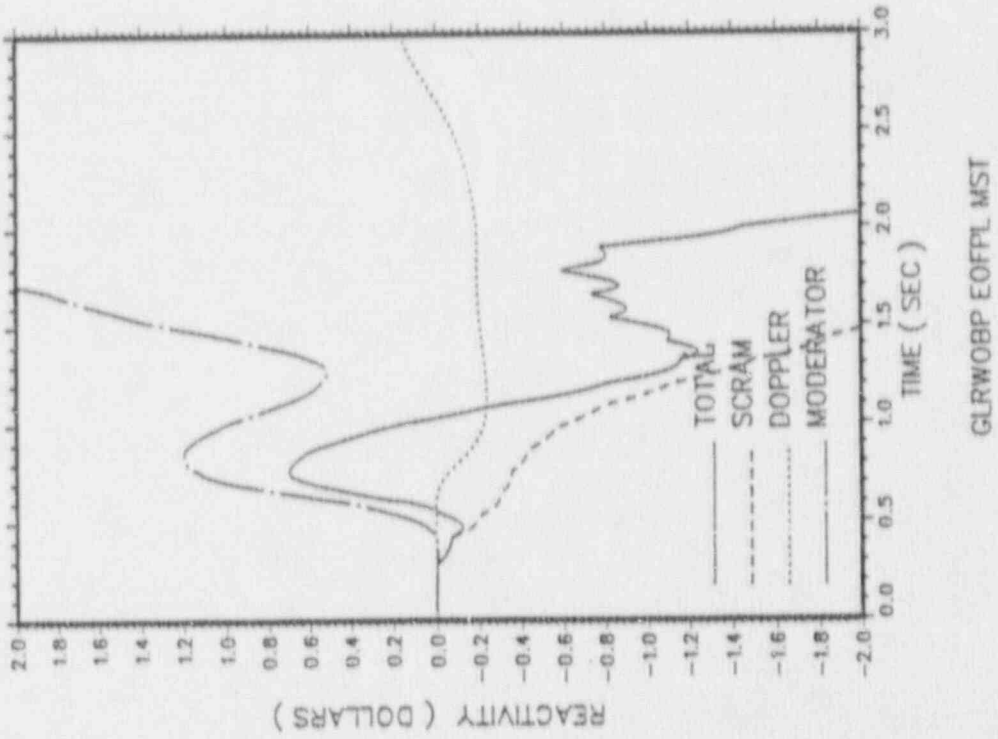

FIGURE 7.2.4-3

Generator Load Rejection Without Bypass, EOFPL15
Transient Response Versus Time, "Measured" Scram Time

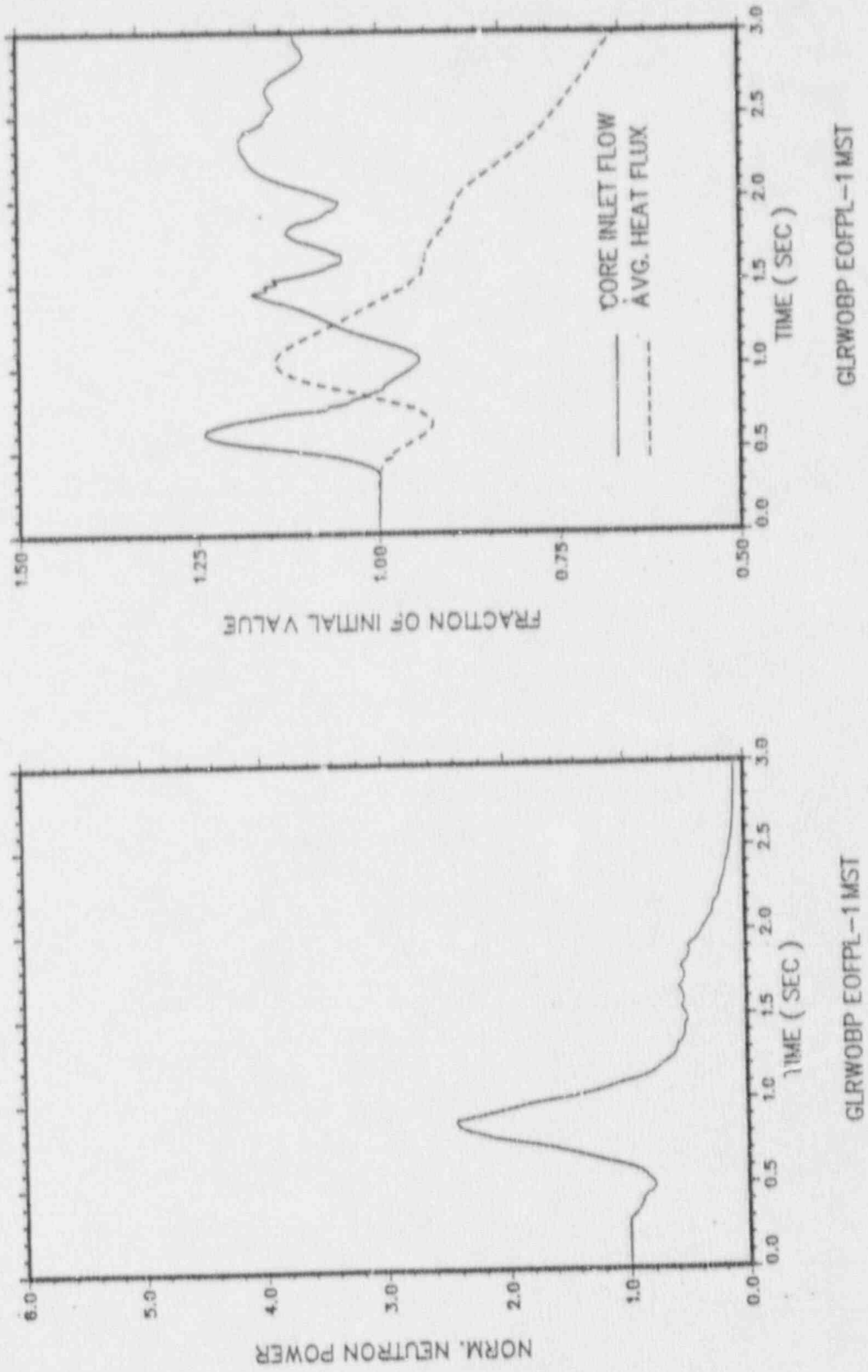

FIGURE 7.2.5-1

Generator Load Rejection Without Bypass, EOFPL15-1000 MWD/ST
Transient Response Versus Time, "Measured" Scram Time

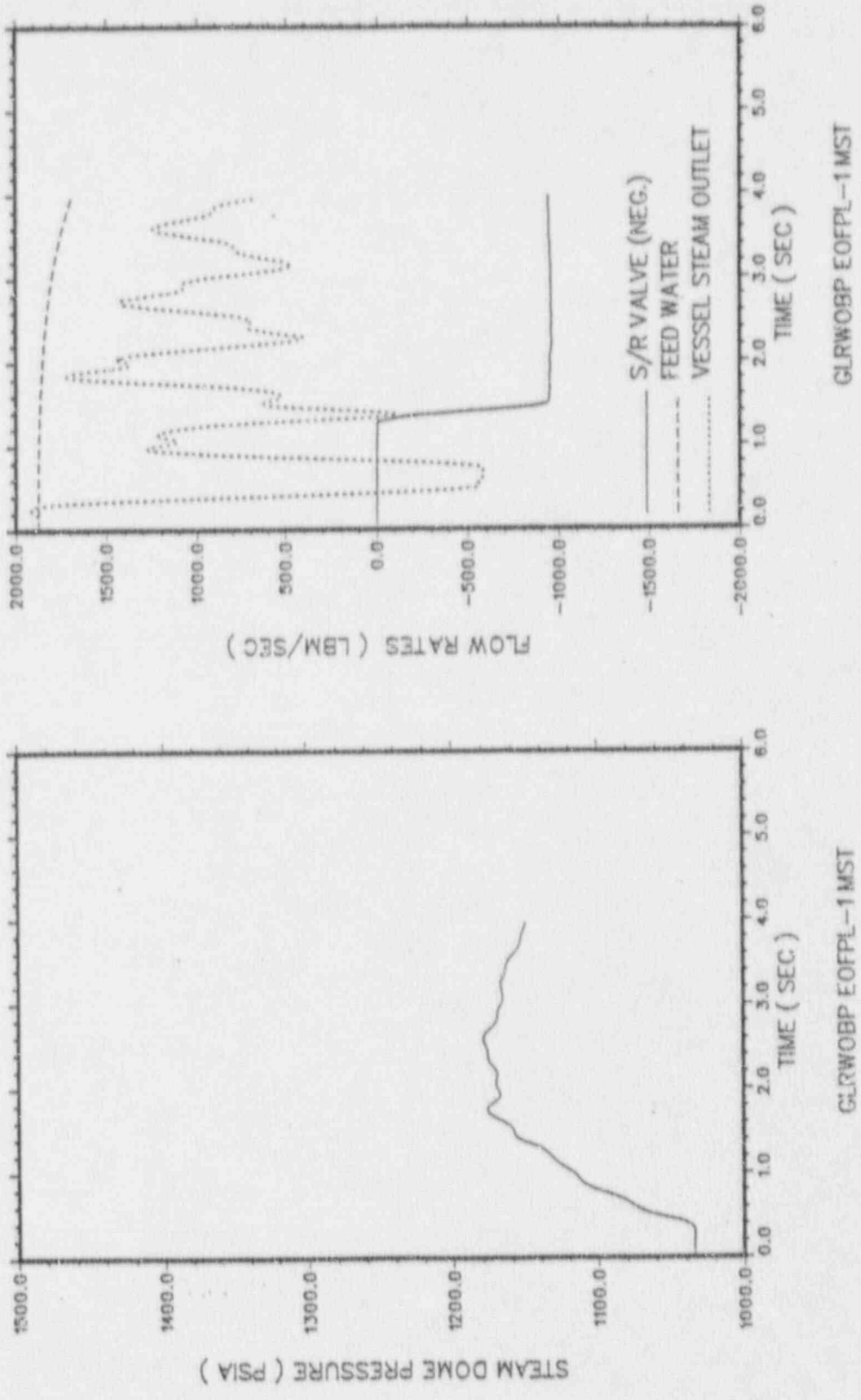

FIGURE 7.2.5-2

Generator Load Rejection Without Bypass, EOFPL15-1000 MWD/ST
Transient Response Versus Time, "Measured" Scram Time

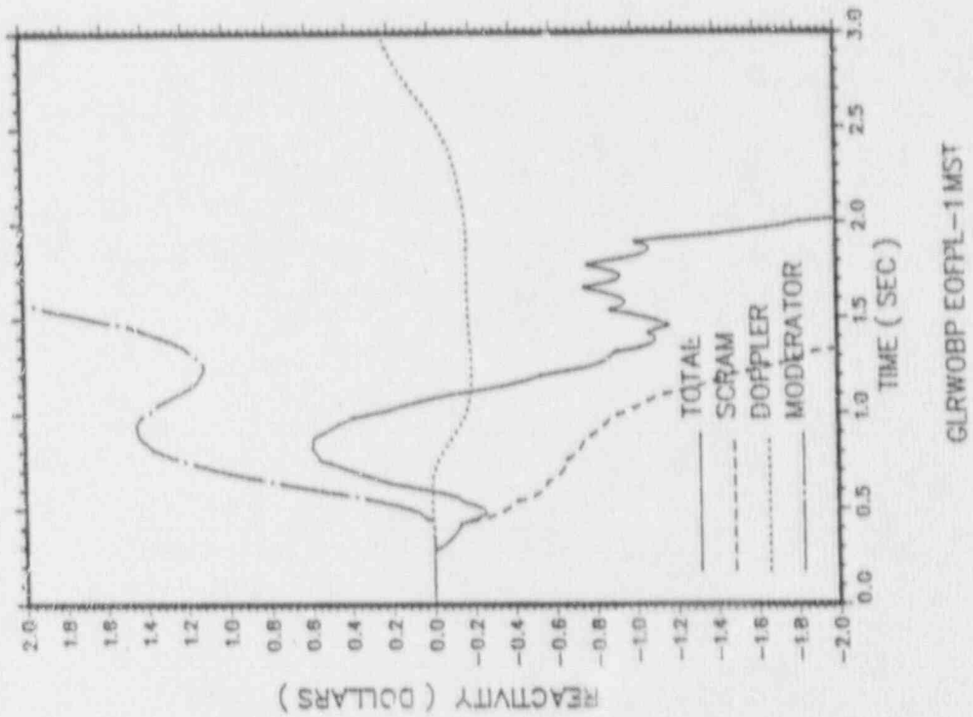

FIGURE 7.2.5-3

Generator Load Rejection Without Bypass, EOFPL15-1000 MWD/ST
Transient Response Versus Time, "Measured" Scram Time

FIGURE 7.2.6-1

Generator Load Rejection Without Bypass, EOFPL15-2000 MWD/ST
Transient Response Versus Time, "Measured" Scram Time

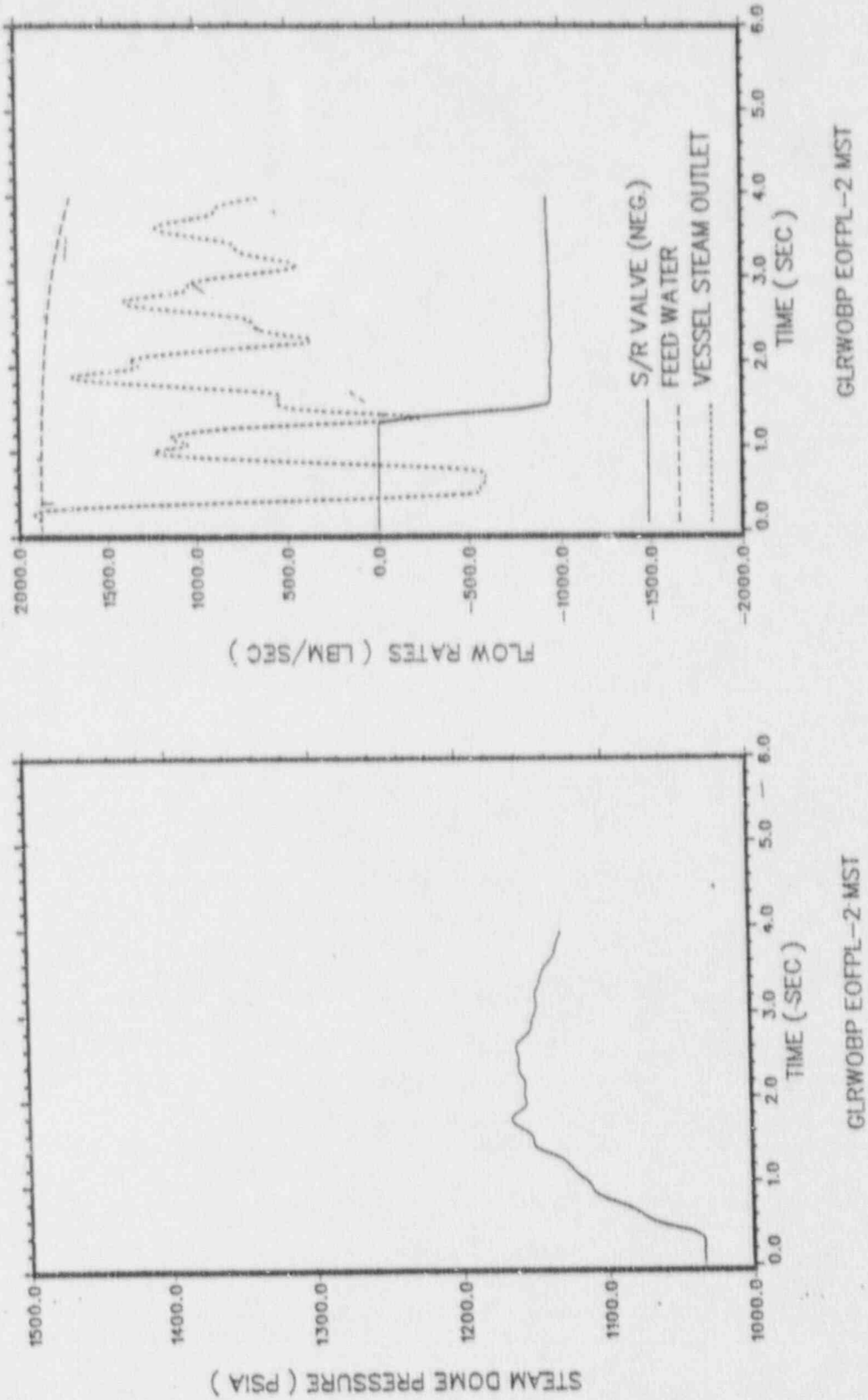

FIGURE 7.2.6-2

Generator Load Rejection Without Bypass, EOFPL15-2000 MWD/ST
Transient Response Versus Time, "Measured" Scram Time

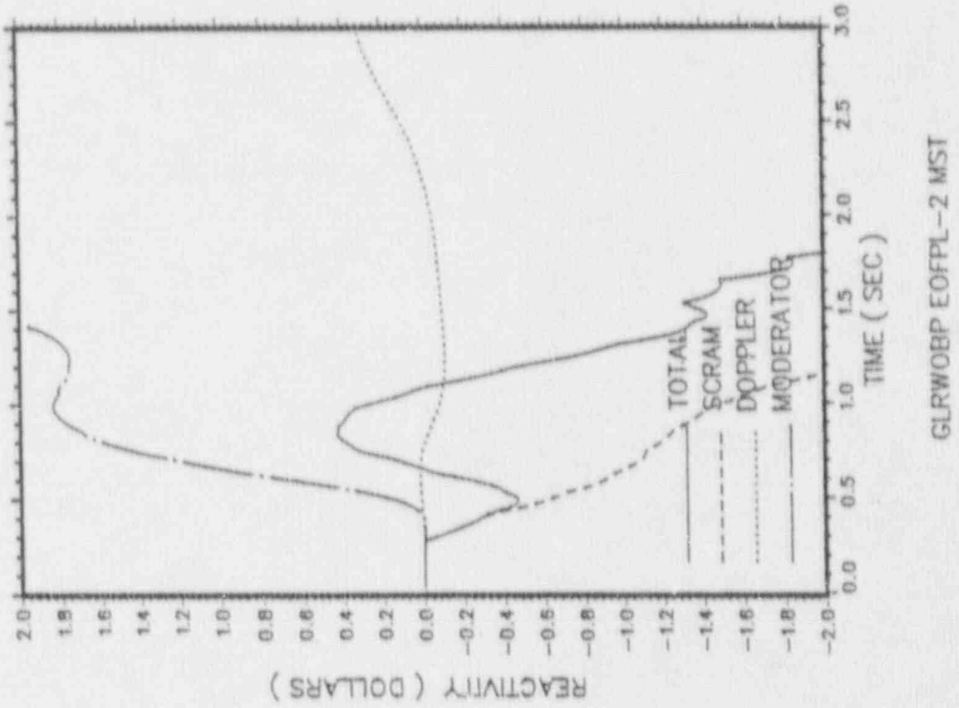

FIGURE 7.2.6-3

Generator Load Rejection Without Bypass, EOFPL15-2000 MWD/ST
Transient Response Versus Time, "Measured" Scram Time

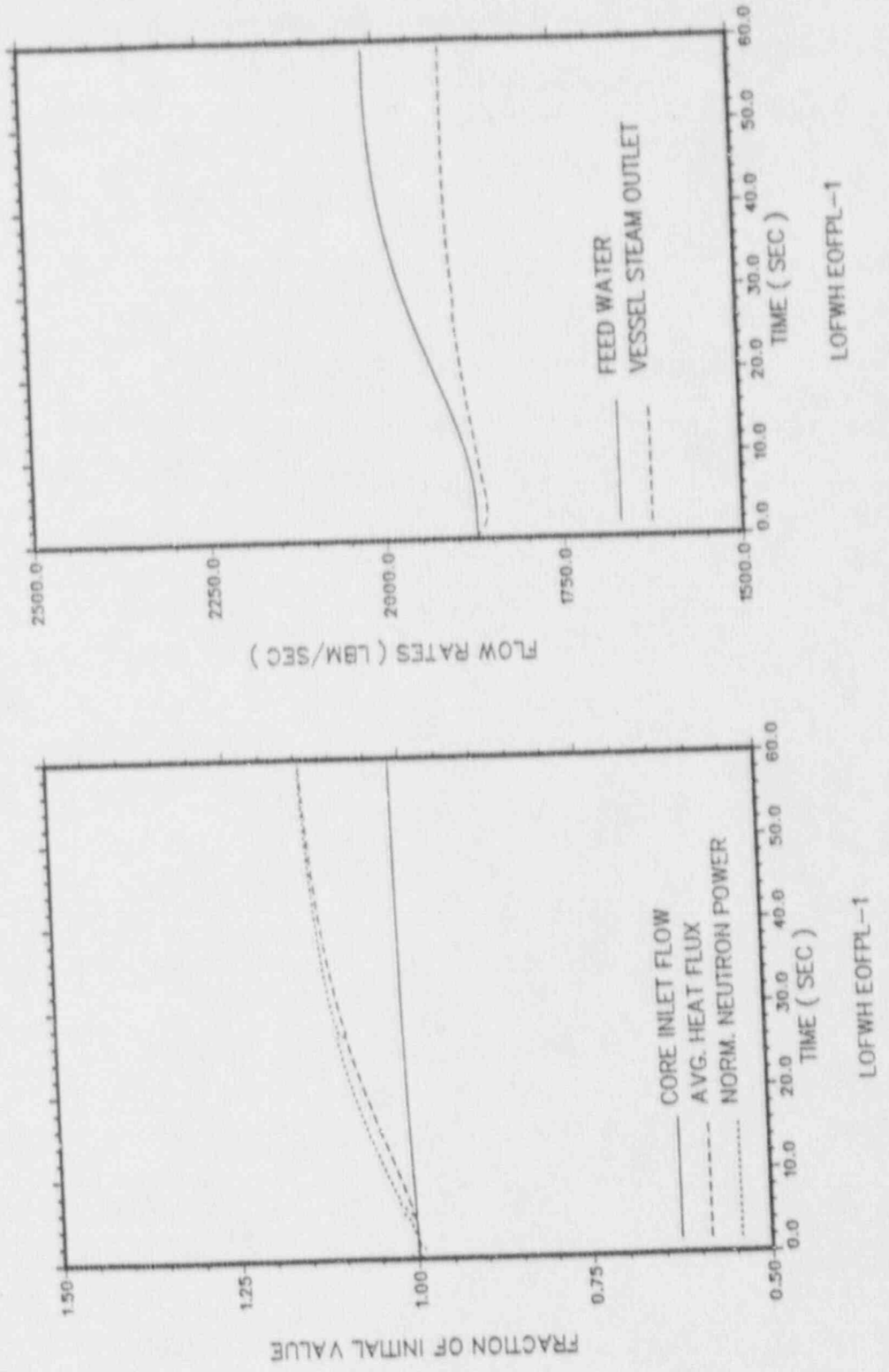

FIGURE 7.2.7-1

Loss of 100°F Feedwater Heating, EOFPL15-1000 MWD/ST (Limiting Case)
Transient Response Versus Time

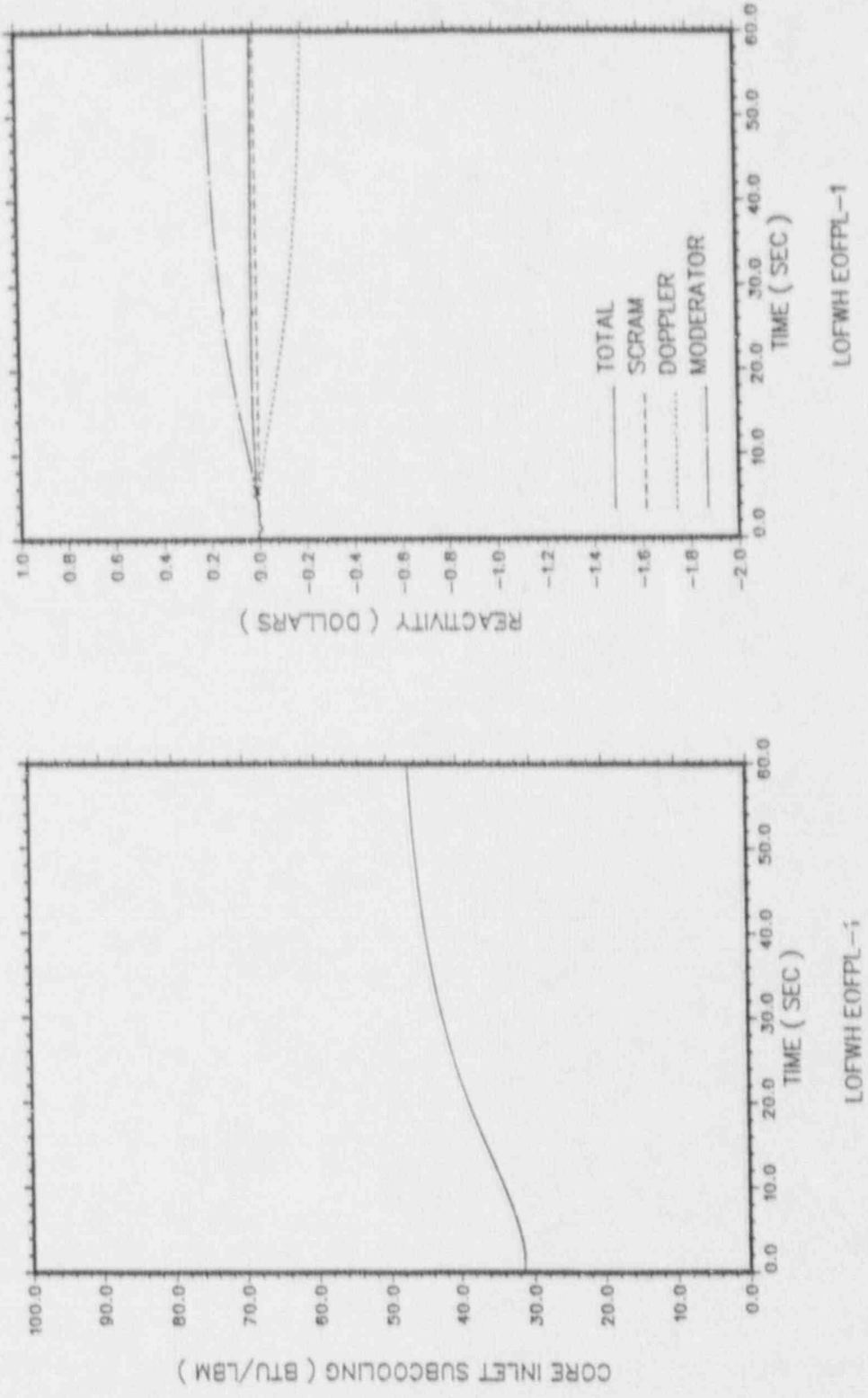

FIGURE 7.2.7-2

Loss of 100°F Feedwater Heating, EOFPL15-1000 MWD/ST (Limiting Case)
Transient Response Versus Time

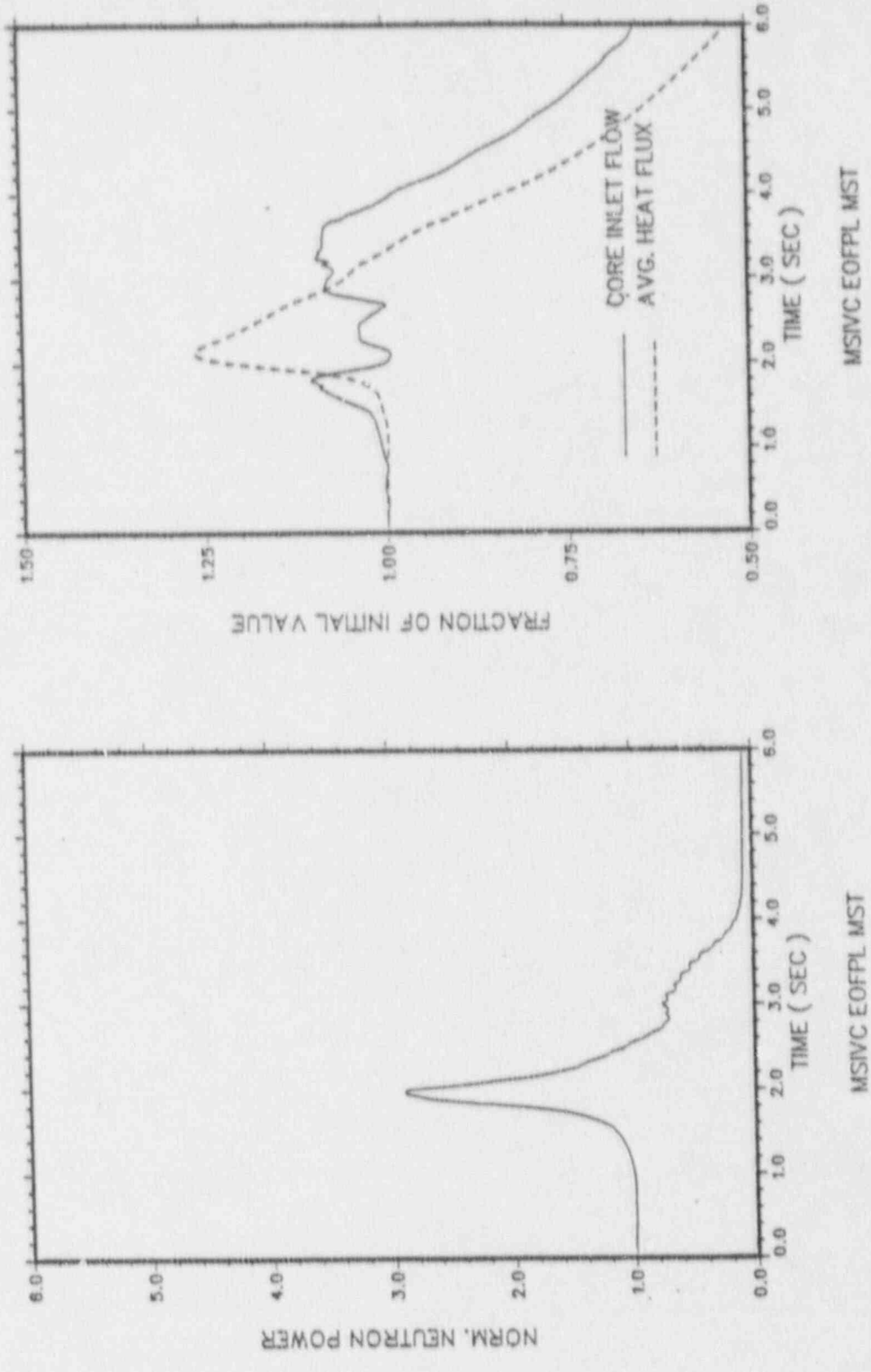

FIGURE 7.3.1-1

MSIV Closure, Flux Scram, EOFPL15
Transient Response Versus Time, "Measured" Scram Time

FIGURE 7.3.1-2

MSIV Closure, Flux Scram, EOFPL15
Transient Response Versus Time, "Measured" Scram Time

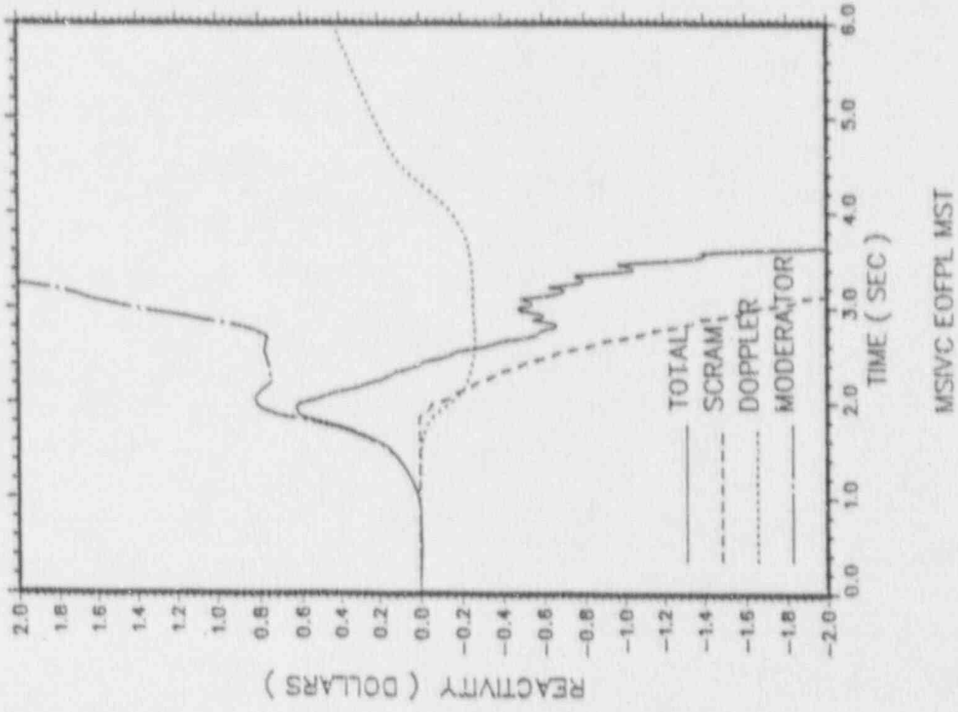

FIGURE 7.3.1-3

MSIV Closure, Flux Scram, EOFPL15
Transient Response Versus Time, "Measured" Scram Time

INITIAL CONDITIONS

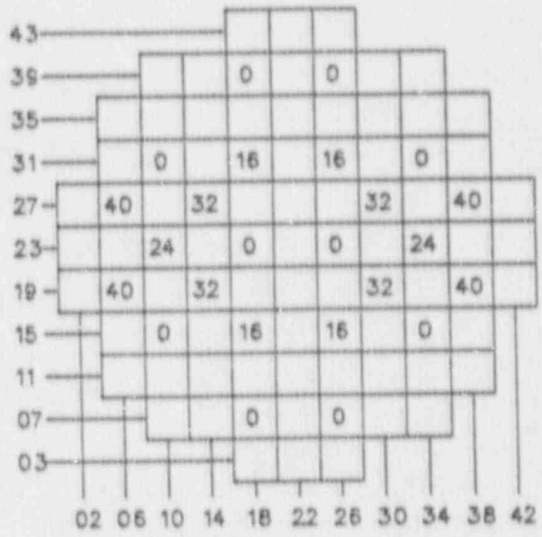

Core Thermal Power = 1864 MWt
Core Flow = 48 Mlb/hr
Cycle Exposure = 6600 MWd/st
Zero Xenon

Core Exit Pressure = 1033 psia
Initial MCPR = 1.384
Initial MLHGR = 14.40 kw/ft
RWE Control Rod = 26-23

TRANSIENT SUMMARY

RBM Setpoint	Rod Position	ΔCPR	MLHGR. (kw/ft)
104	10	0.14	15.41
105	12	0.18	15.97
106	12	0.18	15.97
107	14	0.21	16.57
108	18	0.27	17.79

FIGURE 7.4.1

Reactor Initial Conditions and Transient Summary for the VY Cycle 15 Rod Withdrawal Error Case 1

INITIAL CONDITIONS

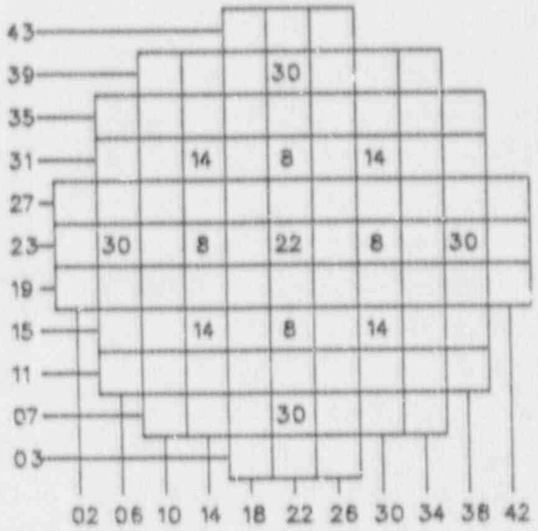

Core Thermal Power = 1664 MWt
Core Flow = 48 Mlb/hr
Cycle Exposure = 5400 MWd/st
Equilibrium Xenon

Core Exit Pressure = 1033 psia
Initial MCPR = 1.587
Initial MLHGR = 11.34 kw/ft
RWE Control Rod = 30-23

TRANSIENT SUMMARY

RBM Setpoint	Rod Position	ΔCPR	MLHGR. (kw/ft)
104	16	0.11	11.35
105	20	0.15	11.38
106	22	0.17	11.39
107	24	0.19	11.44
108	28	0.20	11.57

FIGURE 7.4.2

Reactor Initial Conditions and Transient Summary for the VY Cycle 15 Rod Withdrawal Error Case 2

WFP40/10

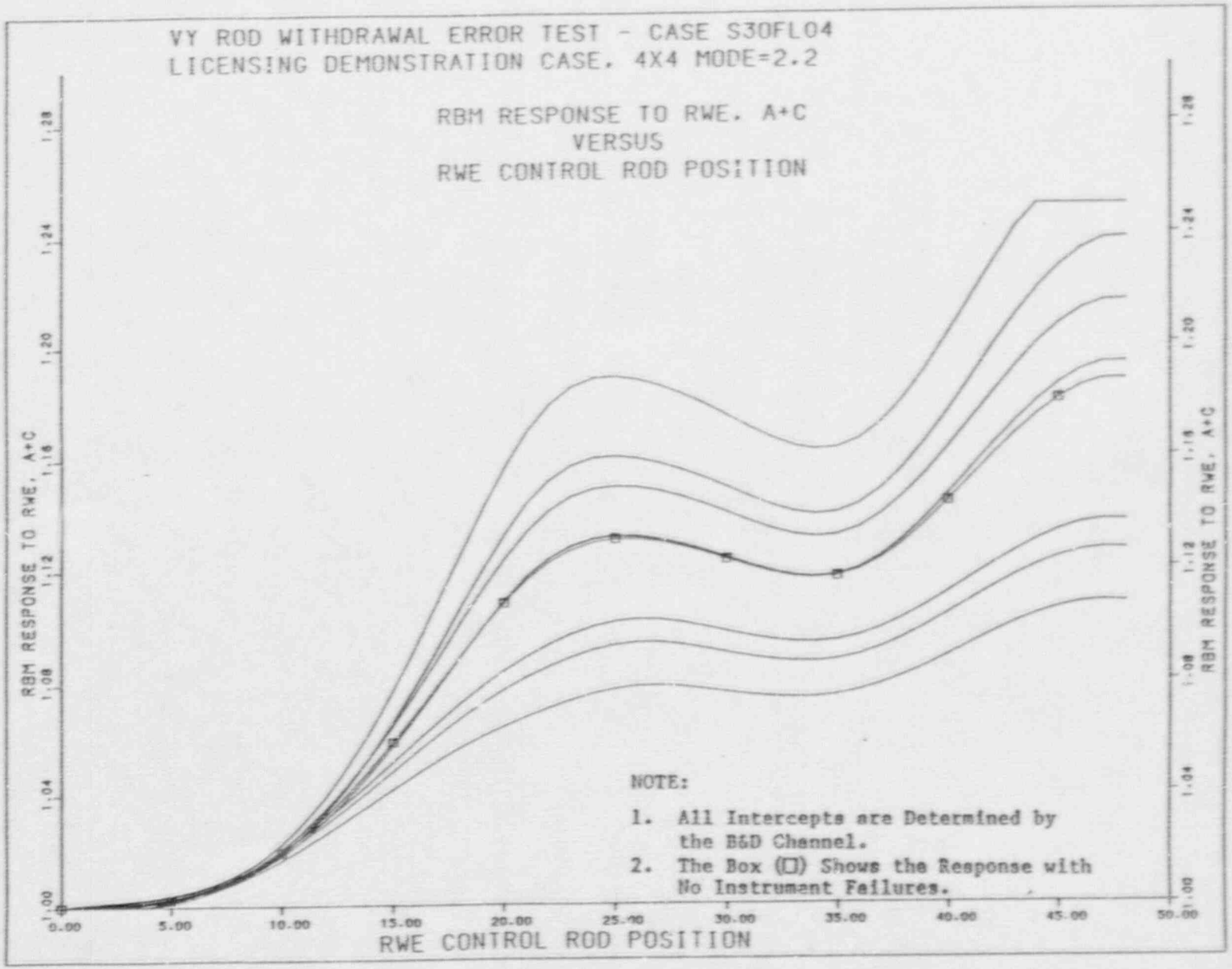

FIGURE 7.4.3

VY Cycle 15 RWE Case 1 - Setpoint Intercepts Determined by the A and C Channels

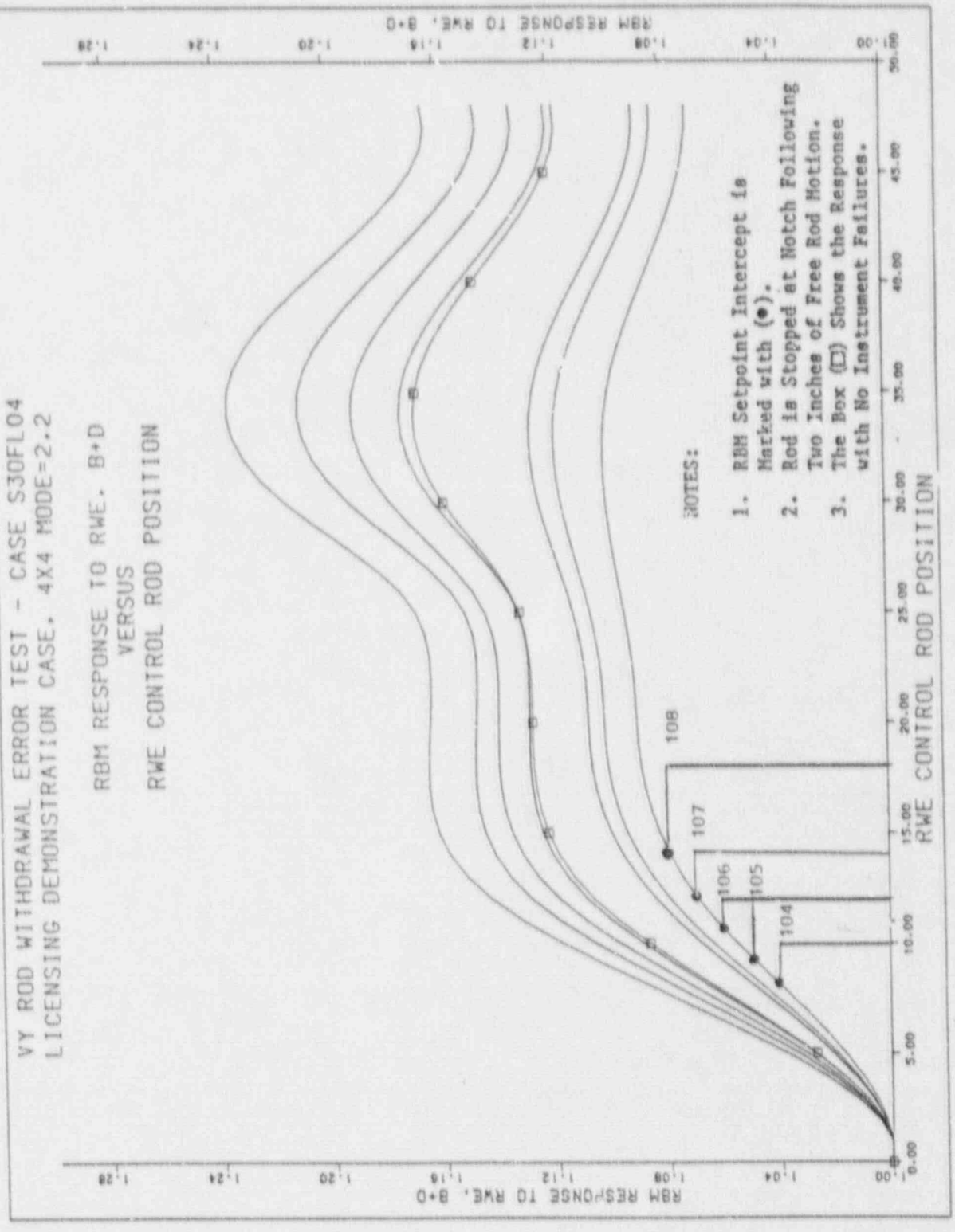

FIGURE 7.4.4

VY Cycle 15 RWE Case 1 - Setpoint Intercepts Determined by the B and D Channels

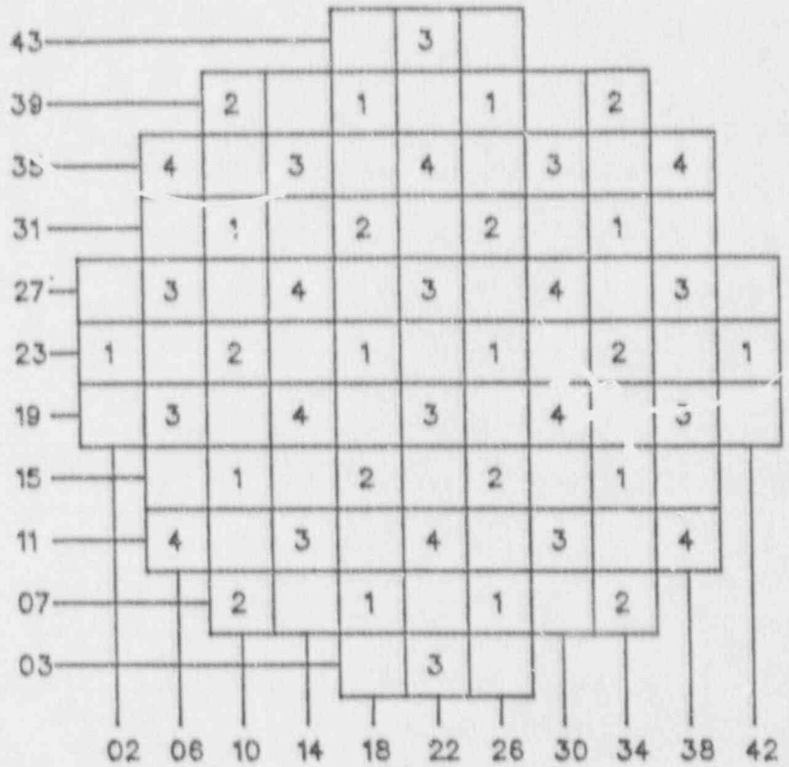

FIGURE 7.6.1

First Four Rod Arrays Pulled in the A Sequences

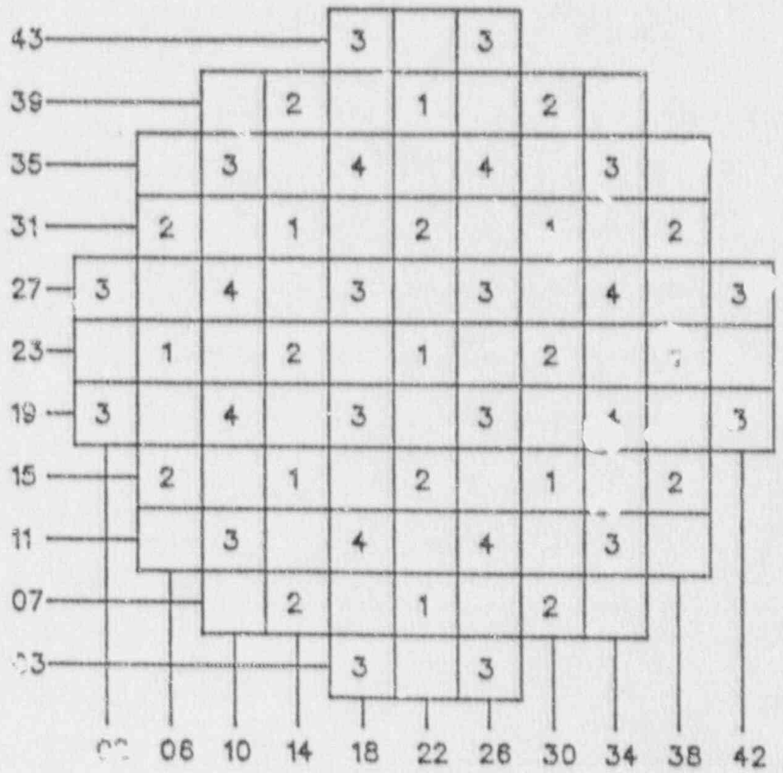

FIGURE 7.6.2

First Four Rod Arrays Pulled in the B Sequences

8.0 LOSS-OF-COOLANT ACCIDENT ANALYSIS

The results of the complete evaluation of the loss-of-coolant accident for Vermont Yankee, as documented in Reference 27, provide the required support for the operation of the Reload Cycle. The LOCA analysis performed in accordance with 10CFR50, Appendix K, demonstrates that the MAPLHGR values comply with the ECCS limits specified in 10CFR50.46. The MAPLHGR limits for all the fuel types in the Reload Cycle, as a function of average planar exposure, are provided in Appendix A. Only the limiting MAPLHGR limits for the zoned fuel are provided in Appendix A. MAPLHGR limits exist for each lattice type and are specified in the process computer.

9.0 CORE COMPONENT QUALIFICATION PROGRAM

9.1 Advanced Nuclear Fuels Fuel Assemblies

Vermont Yankee will be replacing four of the GE BP8DWB311-10GZ bundles with four ANFIX-3.04B-EGZ Qualification Fuel Assemblies (QFAs) [28] to qualify this bundle type for use as a potential reload bundle. The ANF-IX QFAs are manufactured by Advanced Nuclear Fuels Corporation (ANF) and designed to match the GE bundle neutronically and thermal-hydraulically. However, they differ from the GE bundles in the following ways: 1) the average bundle enrichment is lower, at 3.04 w/o U-235; 2) the fuel pins are smaller in diameter and their numbers are higher, at 72; and 3) a large square inner water channel is used rather than a large round water rod. The major mechanical design parameters are given in Table 9.1-1 and in Reference 29.

The bundles will be located at 05-20, 39-20, 05-26, and 39-26. These locations are expected to be nonlimiting with respect to MCPR, MAPLHGR, and MLHGR for the entire cycle. The bundles will be monitored during the cycle to assure that they remain nonlimiting. Reference 30 shows that the use of the ANF bundles does not significantly affect the safety analysis described in Section 7.0. VY specific calculations were also performed to show that the analysis in Section 7.0 bounded the ANF-IX QFAs. Therefore, the ANF-IX QFAs can be monitored as a GE bundle with conservative adjustments to the R-factor tables.

9.2 General Electric Marathon Control Rods

Vermont Yankee will also be replacing eight standard control rods with eight Marathon control rods [31]. These longer-life control blades utilize a combination of B_4C and hafnium as the neutron-absorbing material. Vermont Yankee has approval to use both materials in its control blades [7]. These control rods have been designed to be direct replacement for any of the current GE control rod assemblies. The control rods will be located in nonlimiting locations with respect to shutdown margin. Reference 31 shows that the use of the Marathon control rods does not significantly affect the safety analysis described in Section 7.0.

TABLE 9.1.1

NOMINAL ANF-IX FUEL MECHANICAL DESIGN PARAMETERS

Fuel Bundle*	
Bundle Type	ANF 9X9-IX
Vendor Designation	ANFIX-3.04B-EGZ
Initial Enrichment, w/o U235	3.04
Rod Array	9X9
Fuel Rods per Bundle	72
Outer Fuel Channel	
Material	Zr-2
Wall Thickness, inches	0.080

* Complete bundle, rod, and pellet descriptions found in References 28 and 29.

10.0 STARTUP PROGRAM

Following refueling and prior to vessel reassembly, fuel assembly position and orientation will be verified and videotaped by underwater television.

The Vermont Yankee Startup Program will include process computer data checks, shutdown margin demonstration, in-sequence critical measurement, rod scram tests, power distribution comparisons, TIP reproducibility, and TIP symmetry checks. The content of the Startup Test Report will be similar to that sent to the Office of Inspection and Enforcement in the past [32].

REFERENCES

1. D. J. Morin, Vermont Yankee Cycle 13 Summary Report, YAEC-1680, June 1989.

2. General Electric Standard Application for Reactor Fuel (GESTARII), NEDE-24011-P-A-9, GE Company Proprietary, February 1988, as amended.

3. A. S. DiGiovine, J. P. Gorski, and M. A. Tremblay, SIMULATE-3 Validation and Verification, YAEC-1659-A, September 1988.

4. R. A. Woehlke, et al., MICBURN-3/CASMO-3/TABLES-3/SIMULATE-3 Benchmarking of Vermont Yankee Cycles 9 through 13, YAEC-1683-A, March 1989.

5. VYNPC Letter to USNRC, "Vermont Yankee LOCA Analysis Method: FROSSTEY Fuel Performance Code (FROSSTEY-2)," FVY 87-116, dated December 16, 1987.

6. Loss of Coolant Accident Analysis for Vermont Yankee Nuclear Power Station, NEDO-21697, May 1990, as amended.

7. Appendix A to Operating License DPR-28 Technical Specifications and Bases for Vermont Yankee Nuclear Power Station, Docket No. 50-271.

8. A. S. DiGiovine, et al., CASMO-3G Validation, YAEC-1363-A, April 1988.

9. A. A. F. Ansari, Methods for the Analysis of Boiling Water Reactors: Steady-State Core Flow Distribution Code (FIBWR), YAEC-1234, December 1980.

10. A. A. F. Ansari, R. R. Gay, and B. J. Gitnick, FIBWR: A Steady-State Core Flow Distribution Code for Boiling Water Reactors - Code Verification and Qualification Report, EPRI NP-1923, Project 1754-1 Final Report, July 1981.

11. USNRC Letter to J. B. Sinclair, SER, "Acceptance for Referencing in Licensing Actions for the Vermont Yankee Plant of Reports: YAEC-1232, YAEC-1238, YAEC-1239P, YAEC-1299P, and YAEC-1234," NVY 82-157, September 15, 1982.

12. General Electric Company, GEXL-Plus Correlation Application to BWR 2-6 Reactors GE6 through GE9 Fuel, NEDE-31598P, GE Company Proprietary, July 1989.

13. A. A. F. Ansari and J. T. Cronin, Methods for the Analysis of Boiling Water Reactors: A Systems Transient Analysis Model (RETRAN), YAEC-1233, April 1981.

14. USNRC Letter to R. L. Smith, SER, "Amendment No. 70 to Facility License No. DPR-28," dated November 27, 1981.

WPP40/10

15. V. Chandola, M. P. LeFrancois, and J. D. Robichaud, Appliation of One-Dimensional Kinetics to Boiling Water Reactor Transient Analysis Methods, YAEC-1693-A, Revision 1, November 1989.

16. EPRI, RETRAN - A Program for One-Dimensional Transient Thermal-Hydraulic Analysis of Complex Fluid Flow Systems, CCM-5, December 1978.

17. USNRC Letter to T. W. Schnatz, SER, "Acceptance for Referencing of Licensing Topical Reports: EPRI CCM-5 and EPRI NP-1850-CCM," September 4, 1984.

18. A. A. F. Ansari, K. J. Burns, and D. K. Beller, Methods for the Analysis of Boiling Water Reactors: Transient Critical Power Ratio Analysis (RETRAN-TCPYA01), YAEC-1299P, March 1982.

19. J. T. Cronin, Method for Generation of One-Dimensional Kinetics Data for RETRAN-02, YAEC-1694-A, June 1989.

20. C. J. Paone, et al., Rod Drop Accident Analysis for Large Boiling Water Reactors, NEDO-10527, March 1972.

21. R. C. Stirn, et al., Rod Drop Accident Analysis for Large Boiling Water Reactors Addendum No. 1, Multiple Enrichment Cores With Axial Gadolinium, NEDO-10527, Supplement 1, July 1972.

22. R. C. Stirn, et al., Rod Drop Accident Analysis for Large Boiling Water Reactor Addendum No. 2 Exposed Cores, NEDO-10527, Supplement 2, January 1973.

23. C. J. Paone, Banked Position Withdrawal Sequence, NEDO-21231, January 1977.

24. D. Radcliffe and R. E. Bates, "Reduced Notch Worth Procedure," SIL-316, November 1979.

25. M. A. Sironen, Vermont Yankee Cycle 14 Core Performance Analysis Report, YAEC-1706, October 1988.

26. Final Safety Analysis Report, Vermont Yankee Nuclear Power Station, November 1987.

27. Loss-of-Coolant Accident Analysis for Vermont Yankee Nuclear Power Station, NEDO-21697, August 1977, as amended; NEDE-21697, Supplement 1, November 1987; and NEDE-21697, Supplement 2, May 1990.

28. M. E. Garrett, K. D. Hartley, and M. H. Smith, Vermont Yankee 9X9-IX Qualification Fuel Assembly Design Report, Mechanical, Thermal-Hydraulic, and Neutronic Design, ANF-90-034(P), Revision 0, ANF Company Proprietary, March 1990.

29. Generic Mechanical Designs for Advanced Nuclear Fuels 9X9-IX and 9X9-9X BWR Reload Fuel, ANF-89-014(P), ANF Company Proprietary, May 1989.

30. M. E. Garrett, K. D. Hartley, and M. H. Smith, Vermont Yankee Qualification Fuel Assembly Safety Analysis Report, ANF-90-048, May 1990.

31. GE Marathon Control Rod Assembly, NEDE-31758P, January 1990.

32. R. W. Capstick Letter to W. T. Russell, Regional Administrator, "Cycle 14 Start-Up Test Report," BVY 89-51, dated June 14, 1989.

APPENDIX A

CALCULATED OPERATING LIMITS

The MCPR operating limits for the Reload Cycle are calculated by adding the calculated ΔCPR to the FCISL. This is done for each of the analyses in Section 7.0 at each of the exposure statepoints. For an exposure interval between statepoints, the highest MCPR limit at either end is assumed to apply to the whole interval.

Table A.1 provides the highest calculated MCPR limits for the Reload Cycle for each of the exposure intervals for the various scram speeds and for the various rod block lines.

Tables A.2 through A.6 provide the maximum calculated MAPLHGR limits for all the GE assembly types in the Reload Cycle.

TABLE A.1
(Revised)

VERMONT YANKEE NUCLEAR POWER STATION
CYCLE 15 MCPR OPERATING LIMITS

Value of "N" in RBM Equation (1)	Average Control Rod Scram Time	Cycle Exposure Range	MCPR Operating Limit (2, 3)
42%	Equal or better than L.C.O. 3.3 C.1.1	BOC to EOFPL-2 GWD/T	1.34
		EOFPL-2 GWD/T to EOFPL-1 GWD/T	1.34
		EOFPL-1 GWD/T to EOFPL	1.34
	Equal or better than L.C.O. 3.3 C.1.2	BOC to EOFPL-2 GWD/T	1.34
		EOFPL-2 GWD/T to EOFPL-1 GWD/T	1.34
		EOFPL-1 GWD/T to EOFPL	1.34
41%	Equal or better than L.C.O. 3.3 C.1.1	BOC to EOFPL-2 GWD/T	1.28
		EOFPL-2 GWD/T to EOFPL-1 GWD/T	1.28
		EOFPL-1 GWD/T to EOFPL	1.28
	Equal or better than L.C.O. 3.3 C.1.2	BOC to EOFPL-2 GWD/T	1.28
		EOFPL-2 GWD/T to EOFPL-1 GWD/T	1.28
		EOFPL-1 GWD/T to EOFPL	1.29
≤ 40%	Equal or better than L.C.O. 3.3 C.1.1	BOC to EOFPL-2 GWD/T	1.25
		EOFPL-2 GWD/T to EOFPL-1 GWD/T	1.25
		EOFPL-1 GWD/T to EOFPL	1.25
	Equal or better than L.C.O. 3.3. C.1.2	BOC to EOC-2 GWD/T	1.25
		EOC-2 GWD/T to EOC-1 GWD/T	1.25
		EOC-1 GWD/T to EOC	1.29

NOTES:

(1) The Rod Block Monitor (RBM) trip setpoints are determined by the equation shown in Table 3.2.5 of the Technical Specifications.

(2) The current analysis for the MCPR operating limits does not include the 7X7, 8X8, 8X8R, or P8X8R fuel types. On this basis, if any of these fuel types are to be reinserted, they will be evaluated in accordance with 10CFR50.59 to ensure that the above limits are bounding for these fuel types.

(3) MCPR Operating Limits are increased by 0.01 for single loop operation. Effective 10/90

TABLE A.2

MAPLHGR Versus Average Planar Exposure

Plant: Vermont Yankee

Fuel Type: BP8DRB299

Average Planar Exposure (MWd/St)	MAPLHGR (kW/ft) Two-Loop Operation	MAPLHGR (kW/ft) Single-Loop Operation*
200.0	10.7	8.8
1,000.0	10.8	8.9
5,000.0	11.4	9.4
10,000.0	12.2	10.1
15,000.0	12.3	10.2
20,000.0	12.2	10.1
25,000.0	11.7	9.7
35,000.0	10.6	8.8
41,900.0	9.4	7.8

* MAPLHGR for single-loop operation is obtained by multiplying MAPLHGR for two-loop operation by 0.83.

TABLE A.3

MAPLHGR Versus Average Planar Exposure

Plant: Vermont Yankee

Fuel Type: BD324B

Average Planar Exposure (MWd/St)	MAPLHGR (kW/ft) Two Loop Operation	MAPLHGR (kW/ft) Single-Loop Operation*
200.0	11.22	9.31
3,000.0	11.83	9.81
8,000.0	12.69	10.53
10,000.0	12.80	10.62
15,000.0	12.74	10.57
20,000.0	12.05	10.00
25,000.0	11.39	9.45
35,000.0	10.12	8.39
45,000.0	8.46	7.02
50,000.0	5.99	4.97

* MAPLHGR for single-loop operation is obtained by multiplying MAPLHGR for two-loop operation by 0.83.

TABLE A.4

MAPLHGR Versus Average Planar Exposure

Plant: Vermont Yankee

Fuel Type: BD326B

Average Planar Exposure (MWd/St)	MAPLHGR (kW/ft) Two-Loop Operation	MAPLHGR (kW/ft) Single-Loop Operation*
200.0	11.26	9.34
3,000.0	11.72	9.72
8,000.0	12.76	10.59
10,000.0	12.90	10.70
15,000.0	12.82	10.64
20,000.0	12.12	10.05
25,000.0	11.44	9.49
35,000.0	10.15	8.42
45,000.0	8.63	7.16
50,000.0	6.17	5.12

* MAPLHGR for single-loop operation is obtained by multiplying MAPLHGR for two-loop operation by 0.83.

TABLE A.5

MAPLHGR Versus Average Planar Exposure

Plant: Vermont Yankee

Fuel Type: BP8DWB311-10GZ

Average Planar Exposure (MWd/St)	MAPLHGR (kW/ft) Two-Loop Operation	MAPLHGR (kW/ft) Single-Loop Operation*
200.0	11.00	9.13
6,000.0	11.92	9.89
7,000.0	12.11	10.05
8,000.0	12.34	10.24
10,000.0	12.83	10.64
12,500.0	13.00	10.79
20,000.0	12.24	10.15
25,000.0	11.55	9.58
45,000.0	8.76	7.27
50,740.0	5.91	4.90

* MAPLHGR for single-loop operation is obtained by multiplying MAPLHGR for two-loop operation by 0.83.

TABLE A.6

MAPLHGR Versus Average Planar Exposure

Plant: Vermont Yankee

Fuel Type: BP8DWB311-11GZ

Average Planar Exposure (MWd/St)	MAPLHGR (kW/ft) Two-Loop Operation	MAPLHGR (kW/ft) Single-Loop Operation*
200.0	11.00	9.13
6,000.0	11.92	9.89
7,000.0	12.11	10.05
8,000.0	12.34	10.24
10,000.0	12.83	10.64
12,500.0	12.90	10.70
15,000.0	12.81	10.63
35,000.0	10.24	8.49
45,000.0	8.76	7.27
50,740.0	5.91	4.90

* MAPLHGR for single-loop operation is obtained by multiplying MAPLHGR for two-loop operation by 0.83.